matched NaCl sealed cells on a Perkin-Elmer 283B spectrophotometer equipped with a Data Station and employing the PECDS software package provided by Perkin-Elmer. The spectra were calibrated against a water-vapor spectrum below 2000 cm^{-1} and against a CO spectrum above 2000 cm^{-1}. For recording high-quality infrared spectra an IBM FTIR Model 85 spectrophotometer was used. GC-MS experiments were performed by using a Hewlett-Packard 5710A gas chromatograph coupled to an HP Model 5980 mass spectrometer operating with a Model 5933A data system.

Preparations. $[PPN][\mu\text{-}H(M_2(CO)_{10})]$, where M = Cr and W, were prepared by the procedure reported by Grillone and co-workers.[35] $[PPN][M(CO)_5Cl]$ (M = Cr and W) and $[PPN][Cr(CO)_5O_2CH]$ were synthesized as described previously.[4d,3] $[PPN][W(CO)_5O_2CH]$ and $[PPN][W(CO)_5O_2CCH_3]$ were prepared by reaction of $[PPN][O_2CH]$[4f] or $[PPN][O_2CCH_3]$[4f,36] with $W(CO)_6$ in refluxing DME for 30 min. After removal of DME solvent, THF was added to the yellow solids and the resulting solutions were filtered over celite. Crystals of pure compounds were obtained after addition of hexane to these THF solutions followed by overnight cooling. The complexes were isolated by filtration and dried under vacuum to provide yields of 65–75%. Carbon-13-labeled derivatives $H^{13}CO_2W(CO)_5^-$ and $HCO_2W(^{13}CO)_5^-$ were obtained by our previously published procedure.[3]

Reaction of $[PPN][W(CO)_5O_2CH]$ with Cl_3CCOOH. $[PPN][W(CO)_5O_2CH]$ (0.028 g, 31 μmol) was dissolved in 5 mL of THF under nitrogen followed by addition of 0.0315 g (193 μmol) of Cl_3COOH. The reaction mixture was stirred at ambient temperature and monitored by infrared spectroscopy in the ν(CO) region. After several minutes of reaction the peaks due to the $W(CO)_5O_2CH^-$ anion were shifted to higher frequencies, 1908 and 1844 cm^{-1} shifted to 1913 and 1852 cm^{-1}. The reaction was quantitative as indicated by the intensity of the ν(CO) infrared bands of the products.

Catalytic Reactions. In a typical run, 0.14 mmol of catalyst were dissolved in 15 mL of degassed methanol. After addition of the internal standard (hexane), the solution was placed inside a dry box and transferred to a 300-mL Parr reactor. This vessel was then removed from the dry box and pressurized up to 250 psi (at 25 °C) with pure CO_2. Molecular hydrogen was used to carry the pressure up to 500 psi. The reactor was heated by means of the mantle equipped with a Parr temperature controller Model 4831. When the temperature inside the reactor (measured with a thermocouple type J (Iron–constantan)) reached 125 °C, the clock was started. At the end of the reaction period (normally 24 h) the heating was discontinued and the reactor placed in an ice bath for 1 h. At this moment a gas sample was taken by allowing the gas to escape and collecting it using a glass sampling device. After putting the reactor inside a dry box, the vessel was opened and the reaction solution transferred to the IR cell and to a septum-capped vial in order to be analyzed by GC (Perkin-Elmer Model Sigma 2 equipped with a thermo-conductivity detector and a Cole-Palmer recorder Model 8385-32, the column used for analyses of liquid samples was 10% carbowax 20 m over chromosorb (2 m × $^1/_8$ in.), 50 °C (1 min) to 130 °C at 25 °C/min, inlet pressure 21 psi of He; for gas samples the column used was carbosphere, 100 °C (1.5 min) to 160 °C (2 min) at 25 °C/min).

The high-pressure infrared measurements were carried out with use of the same Parr reactor as well as the same loading procedures. The high-pressure IR cell (CIR cell) used was provided by Barnes Analytical. The reactor was connected to the cylindrical internal reflection cell by means of $^1/_{16}$-in. tubing, and the sample was delivered directly from the reactor to the cell with both being maintained at the pressure of the reactor. Background spectra were determined in a completely analogous manner in the absence of catalyst.

Acknowledgment. The financial support of this research by the National Science Foundation (Grant CHE 83-08281) is greatly appreciated.

Registry No. $\mu\text{-}H[W_2(CO)_{10}]^-PPN^+$, 56172-01-1; $HCO_2W(CO)_5^-PPN^+$, 36499-81-7; $W(CO)_6$, 14040-11-0; $ClW(CO)_5^-PPN^+$, 39048-34-5; $CH_3CO_2W(CO)_5^-PPN^+$, 36515-92-1; $\mu\text{-}H[Cr_2(CO)_{10}]^-PPn^+$, 62314-83-7; $HCO_2Cr(CO)_5^-PPn^+$, 82880-57-7; HC(O)OMe, 107-31-3; CO_2, 124-38-9; HC(O)OEt, 109-94-4; H_2, 1333-74-0; $H^{13}CO_2W(CO)_5^-$, 90065-85-3; $HCO_2W(^{13}CO)_5^-$, 90065-86-4.

---

[35] Grillone, M. D.; Kedzin, B. B. *J. Organomet. Chem.* **1977**, *140*, 161.

[36] Martinsen, A.; Songstad, J. *Acta Chem. Scand., Ser. A* **1977**, *A31*, 645.

Synthesis of a Chelated Tungsten–Carbene–Alkene Complex and Its Conversion to a Cyclopropane

Charles P. Casey,* Nicholas W. Vollendorf, and Kenneth J. Haller

Contribution from the Department of Chemistry, University of Wisconsin, Madison, Wisconsin 53706. *Received September 16, 1983*

Abstract: Reaction of $(CO)_5W{=}C(OCH_3)C_6H_4\text{-}p\text{-}CH_3$ with 1-amino-2,2-dimethyl-3-butene (**8**) gave a 3:1 mixture of the *Z* and *E* isomers of pentacarbonyl [((2,2-dimethyl-3-butenyl)amino)(*p*-tolyl)carbene]tungsten(0) (**10**-*Z* and **10**-*E*). Thermolysis of **10** did not produce a metal–carbene–alkene complex but rather led to formation of an imine decomposition product. N-Methylation of **10** by treatment with lithium diisopropylamide and methyl iodide produced a mixture of the *Z* and *E* isomers of pentacarbonyl [((*N*,2,2-trimethyl-3-butenyl)amino)(*p*-tolyl)carbene]tungsten(0) (**13**-*Z* and **13**-*E*). Thermolysis of **13** in benzene at 88 °C led to formation of the tungsten–carbene–alkene complex tetracarbonyl[(((*Z*)-η^2-*N*,2,2-trimethyl-3-butenyl)amino)(*p*-tolyl)carbene]tungsten(0) (**6**). Further heating of **6** gave the cyclopropane 1-*p*-tolyl-2,4,4-trimethyl-2-azabicyclo[3.1.0]hexane (**7**). The X-ray crystal structure of **6** shows two independent molecules per unit cell; in one molecule, the carbene and alkene ligands are approximately parallel and in the other they are approximately perpendicular. Crystal data for **6**: space group $P2_1$, $Z = 4$, $a = 10.287$ (3) Å, $b = 11.651$ (3) Å, $c = 16.319$ (5) Å, $\beta = 98.83$ (2)°, $R = 0.039$, and $R_w = 0.053$ for the 4295 reflections with $F_o > 3\sigma(F_o)$. ^{1}H NMR of **6** revealed fluctional processes attributed to slow rotation of the *p*-tolyl group and to reversible decomplexation of the alkene ligand of **6**. PPh_3 reversibly displaces the alkene ligand of **6** and also accelerates cyclopropane formation from **6**.

Metal–carbene–alkene complexes have been proposed as important intermediates in the olefin metathesis reaction,[1] in the cyclopropanation[2] of alkenes, and in Ziegler–Natta polymerization of alkenes.[3] Examples of chelated[4-9] and nonchelated[10,11] metal–carbene–alkene complexes are known, but most of these com-

---

[1] Grubbs, R. H. *Prog. Inorg. Chem.* **1978**, *24*, 1–50. Katz, T. J. *Adv. Organomet. Chem.* **1977**, *16*, 283–317. Calderon, N.; Lawrence, J. P.; Ofstead, E. A. *Ibid.* **1979**, *17*, 449–492.

[2] Nozaki, H.; Moriuti, S.; Takaya, H.; Noyori, R. *Tetrahedron Lett.* **1966**, 5239–5244. Nozaki, H.; Takaya, H.; Moriuti, S.; Noyori, R. *Tetrahedron* **1968**, *24*, 3655–3669. Moser, W. R. *J. Am. Chem. Soc.* **1969**, *91*, 1135–1140, 1141–1146.

0002-7863/84/1506-3754$01.50/0

plexes do not take part in either olefin metathesis or cyclopropanation reactions.

The only direct evidence for the conversion of a metal–alkene–carbene complex into a metallacyclobutane or a metallacyclobutane decomposition product is our recent discovery of a series of (alkenyloxy)carbene complexes of tungsten which decompose to cyclopropanes.[12] In the autocatalytic decomposition of $(CO)_5W[C(OCH_2CH_2CH{=}CH_2)C_6H_4\text{-}p\text{-}CH_3]$ (**1**) two different tetracarbonyltungsten–carbene–alkene intermediates were detected by NMR and IR spectroscopy, both of which decomposed to cyclopropane **2**. The two carbene–alkene complexes are thought to differ in the relative orientations of the carbene and alkene ligands; the M=C and C=C bonds can be either parallel or perpendicular.

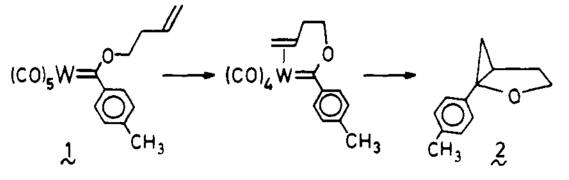

The greater electron-donor ability of nitrogen stabilizes amino-substituted carbene complexes compared with their alkoxy-substituted analogues. We took advantage of this nitrogen stabilization in the synthesis of the very stable amino-substituted metal–carbene–alkene complex **3**.[13] While complex **3** is thermally stable to over 100 °C and has been characterized by X-ray crystallography, it does not decompose to either cyclopropanes or olefin metathesis products. This is attributed to the reluctance to form a highly strained bicyclo[2.2.0] metallacycle which would be the precursor of either the bicyclo[2.1.0] system of the cyclopropane or the azacyclobutene ring of the alkene scission product.

Since the (butenyloxy)carbene complex **1** gave cyclopropane **2** upon thermal decomposition, we began studies of (butenylamino)carbene complexes in an effort to prepare an isolable metal–carbene–alkene complex that would also be a cyclopropane precursor. However, thermolysis of (butenylamino)carbene complex **4**, in which the alkene unit is not coordinated to tungsten, led to double bond isomerization and isolation of the substituted (allylamino)carbene–alkene complex **5** similar to **3**. Apparently, a chelate system with two atoms joining the carbene and alkene ligands is particularly stable.

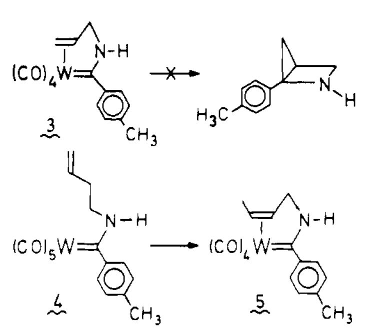

Here we report that when alkene isomerization is blocked by allylic methyl substitution, the stable (butenylamino)carbene–alkene–tungsten complex **6** can be isolated and characterized by X-ray crystallography. Moreover, extended heating of **6** leads to the formation of cyclopropane **7**.

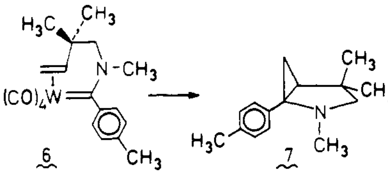

Results

Pentacarbonyl[((2,2-dimethyl-3-butenyl)amino)(*p*-tolyl)carbene]tungsten(0). Our first attempt to prepare a (butenylamino)carbene complex in which alkene isomerization was blocked utilized 1-amino-2,2-dimethyl-3-butene (**8**). Dimethylation of 3-butenenitrile was achieved by two in situ LDA deprotonation–CH_3I alkylation sequences and gave 2,2-dimethyl-2-butenenitrile (**9**) in 33% yield.[14] Reduction of **9** with $LiAlH_4$–$AlCl_3$ gave the desired primary amine **8** in 43% yield.

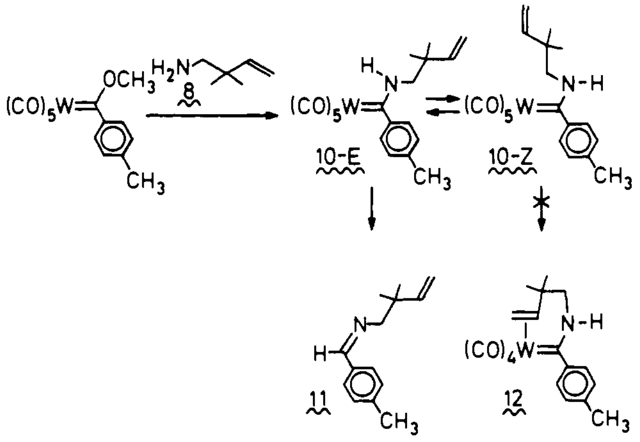

Addition of **8** to a red ether solution containing a small excess of $(CO)_5W{=}C(OCH_3)C_6H_4\text{-}p\text{-}CH_3$ led to instantaneous formation of a yellow-orange solution from which **10** was isolated by column chromatography in 63% yield as a waxy yellow solid. ^1H and ^{13}C NMR spectroscopy indicated that the solid consisted of a 3:1 mixture of two isomers, **10**-*Z* and **10**-*E*, which differed in the orientation of the alkyl group about the carbene carbon–nitrogen partial double bond. Amino-substituted carbene complexes have a high barrier to rotation about the carbene carbon–nitrogen bond that has been attributed to π bonding between carbon and nitrogen and contributions from resonance structures such as $^-MCR{=}NR_2{}^+$. The major isomer was assigned the *Z* configuration based on Fischer's observations that the ^1H NMR resonances of an alkyl group cis to the metal (*Z* isomers) in aminocarbene complexes always appear downfield of those trans to the metal (*E* isomers).[15,16] We have confirmed Fischer's assignments for several cases[13] where interconversion between *Z* isomers and chelated metal–carbene–alkene complexes have allowed definitive assignments. The downfield NCH_2 resonance

---

(3) Ivin, K. J.; Rooney, J. J.; Stewart, C. D.; Green, M. L. H.; Mahtab, R. *J. Chem. Soc., Chem. Commun.* **1978**, 604–606.

(4) Mitsudo, T.; Nakanishi, H.; Inubushi, I.; Morishima, I.; Watanabe, Y.; Takegami, Y. *J. Chem. Soc., Chem. Commun.* **1976**, 416–417. Mitsudo, T.; Watanabe, Y.; Nakanishi, H.; Morishima, I.; Inubushi, T.; Takegami, Y. *J. Chem. Soc., Dalton Trans.* **1978**, 1298–1304. Nakatsu, K.; Mitsudo, T.; Nakanishi, H.; Watanabe, Y.; Takegami, Y. *Chem. Lett.* **1977**, 1447–1448.

(5) Nesmeyanov, A. N.; Sal'nikova, T. N.; Struchkov, Yu. T.; Andrianov, V. G.; Pogrebnyak, A. A.; Rybin, L. V.; Rybinskaya, M. I. *J. Organomet. Chem.* **1976**, *117*, C16–C20.

(6) Aumann, R.; Wormann, H.; Kruger, C. *Angew. Chem., Int. Ed. Engl.* **1976**, *15*, 609–610.

(7) Hiraki, K.; Sugino, K.; Onishi, M. *Bull. Chem. Soc. Jpn.* **1980**, *53*, 1976–1981. Hiraki, K.; Sugino, K. *J. Organomet. Chem.* **1980**, *201*, 469–475.

(8) Dobrzynski, E. D.; Angelici, R. J. *Inorg. Chem.* **1975**, *14*, 1513–1518.

(9) Toledano, C. A.; Levisalles, J.; Rudler, M.; Rudler, H.; Daran, J.-C.; Jeannin, Y. *J. Organomet. Chem.* **1982**, *228*, C7–C11.

(10) Priester, W.; Rosenblum, M. *J. Chem. Soc., Chem. Commun.* **1978**, 26–27.

(11) Schultz, A. J.; Brown, R. K.; Williams, J. M.; Schrock, R. R. *J. Am. Chem. Soc.* **1981**, *103*, 169–176.

(12) A preliminary communication has appeared: Casey, C. P.; Shusterman, A. J. *J. Mol. Catal.* **1980**, *8*, 1–13. See also: Casey, C. P.; Shusterman, A. J.; Scheck, D. M. *Fundam. Res. Homogeneous Catal.* **1979**, *3*, 141–150.

(13) Casey, C. P.; Shusterman, A. J.; Vollendorf, N. W.; Haller, K. J. *J. Am. Chem. Soc.* **1982**, *104*, 2417–23.

(14) Brenner, S.; Bovete, M. *Tetrahedron* **1975**, *31*, 153–158.

(15) Moser, E.; Fischer, E. O. *J. Organomet. Chem.* **1969**, *16*, 275–282.

(16) Fischer, E. O.; Leupold, M. *Chem. Ber.* **1972**, *105*, 599–608.

at δ 3.91 was assigned to major isomer **10**-*Z* while the NCH_2 resonance at δ 3.15 was assigned to **10**-*E*. The normal positions of the vinyl hydrogen resonances and of the alkene carbon resonances in the ^1H and ^{13}C NMR spectra of **10**-*Z* and **10**-*E* indicate that the alkene groups are not coordinated to tungsten.

The major thermal reactions of **10** are *Z*–*E* isomerization and decomposition to imine **11**; no formation of a metal–carbene–alkene complex **12** was observed. When a 3:1 mixture of **10**-*Z*:**10**-*E* in benzene-d_6 was heated at 126 °C for 13 h, the ^1H NMR of the reaction mixture indicated that the 2,2-dimethyl-3-butenylimine of *p*-tolualdehyde, **11**, was formed in 26% yield and that the 35% remaining carbene complex **10** had isomerized to a 1.0:1.3 mixture of *Z* and *E* isomers. After 40 h at 126 °C, less than 5% of **10** remained and the yield of **11** had risen to 38%. At least three other minor products were present, as indicated by resonances for *p*-tolyl groups. Weak signals in the δ 3.25–2.25 region suggested that one of these minor products might contain a coordinated alkene. However, the desired tungsten–carbene–alkene complex **12** was never isolated or unambiguously identified in solution.

Z–*E* isomerization and imine formation were seen as side reactions in the conversions of an (allylamino)carbene complex to metal–carbene–alkene complex **3** and occurred under conditions similar to those employed here. We believe that the desired metal–carbene–alkene complex **12** may be formed reversibly and that starting material **10** is eventually drained off to imine **11**. The larger ring chelate of the desired metal–carbene–alkene complex **12** is apparently less stable than the smaller chelate of the allylamino complex **3** as evidenced by isomerization of the unblocked butenylamino carbene complex **4** to the smaller ring chelate **5**[13] and also by the rapid dissociation of the coordinated alkene of the (butenylamino)carbene complex **6** to be described later.

Attempted generation of tungsten–carbene–alkene complex **12** by photolysis at 350 nm led to rapid *Z*–*E* photoisomerization to give a 1:2 photostationary state of **10**-*Z*:**10**-*E* and slower formation of imine **11**. No evidence for tungsten–carbene–alkene complex **12** was obtained. Similar photochemical *Z*–*E* isomerization was seen previously.[13]

Pentacarbonyl[((*N*,2,2-trimethyl-3-butenyl)amino)(*p*-tolyl)carbene]tungsten(0). Imine formation in the thermolysis of aminocarbene complexes can be base catalyzed and occurs only for aminocarbene complexes with N–H bonds.[17] Imine formation probably proceeds via rapid reversible deprotonation of the N–H group and occasional protonolysis of the W–C bond of the resulting anion. To block imine formation, we decided to methylate the nitrogen atom of aminocarbene complex **10**.

Treatment of aminocarbene complex **10** with 1.1 equiv of lithium diisopropylamide (LDA) in THF at −72 °C followed by warming to room temperature and addition of 1.3 equiv of CH_3I at −72 °C led to clean N-methylation.[18] Pentacarbonyl[((*N*,2,2-trimethyl-3-butenyl)amino)(*p*-tolyl)carbene]tungsten(0) (**13**) was isolated as a viscous yellow oil in 85% yield after column chromatography. The *Z*:*E* ratios varied from 9:1 to 3:1. The *Z* configuration was assigned to the major isomer since its NCH_2 resonance appears at δ 3.88, downfield from the δ 2.81 NCH_2 resonance of **13**-*E*, and since its NCH_3 resonance appears at δ 2.20, upfield from the δ 3.29 NCH_3 resonance of **13**-*E*. This assignment was later confirmed by interconversion of **13**-*Z* and metal–carbene–alkene complex **6**. The ^1H and ^{13}C resonances of the alkene portions of **13**-*Z* and **13**-*E* clearly indicated that the alkene was not complexed to tungsten. The infrared spectrum of the mixture of **13**-*Z* and **13**-*E* exhibits the characteristic pattern for a $(CO)_5MX$ molecule with peaks at 2055 (m), 1975 (w), 1936 (vs), and 1910 (sh) cm^{-1}.

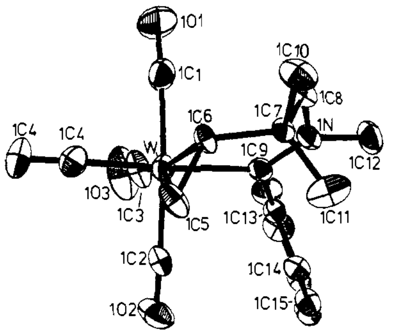

Figure 1. ORTEP drawing of molecule 1 of **6** showing the perpendicular orientation of its carbene and alkene ligands.

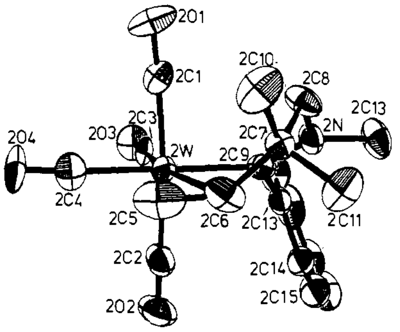

Figure 2. ORTEP drawing of molecule 2 of **6** showing the parallel orientation of its carbene and alkene ligands.

This N-methylation procedure was also used to convert **3** to **14** in 94% yield.

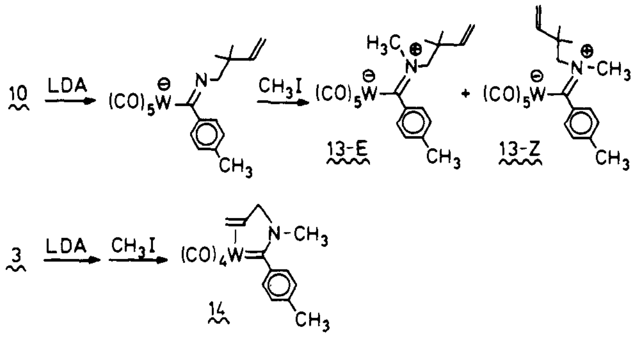

Conversion of 13 to a Chelated Metal–Carbene–Alkene Complex and on to a Cyclopropane. Thermolysis of a 2:1 mixture of **13**-*Z*:**13**-*E* in benzene-d_6 at 99 °C for 75 h led to the formation of chelated metal–carbene–alkene complex **6** in 35% yield and of cyclopropane **7** in 18% yield and to the reisolation of starting material **13** with a 1:3.5 *Z*:*E* ratio. Metal–carbene–alkene complex **6** was characterized spectrally and by X-ray crystallography. The spectral determination of the conformational equilibrium of **6** will be presented after discussion of its X-ray structure.

Cyclopropane **7** was purified by thin-layer chromatography and vacuum distillation. In the 270-MHz ^1H NMR spectrum of **7**, the cyclopropyl protons constitute an isolated AMX pattern consisting of three doublets of doublets at δ 0.79 (J_{gem} = 5.9 Hz, J_{cis} = 8.3 Hz), 0.89 (J_{gem} = 5.9 Hz, J_{trans} = 4.6 Hz), and 1.00 (J_{cis} = 8.3 Hz, J_{trans} = 4.6 Hz). The nonequivalent NCH_2 protons appear as two doublets at δ 2.61 and 1.67 (J_{gem} = 9.7 Hz). The nonequivalent ring methyl groups appear as two singlets at δ 1.22 and 0.93. In the ^{13}C NMR of **7**, the cyclopropyl CH_2 resonances appears as a triplet at δ 5.3 (J = 137 Hz).

Solid-State Structure of Tungsten–Carbene–Alkene Complex 6. The X-ray crystal structure of **6** revealed two independent molecules in the unit cell which have different conformations of the chelating carbene–alkene ligand. In molecule 1 shown in Figure 1, the carbene carbon–tungsten bond and the alkene carbon–carbon double bond are approximately perpendicular. In molecule 2 (Figure 2), these bonds are approximately parallel.

---

(17) Conner, J. A.; Rose, P. D. *J. Organomet. Chem.* **1972**, *46*, 329–334.

(18) In the course of developing this N-methylation procedure, we found that when **10** was subjected to two in situ LDA deprotonation–CH_3I alkylation sequences that some *N*-ethylaminocarbene complex $(CO)_5W{=}C[N(CH_2CH_3)CH_2C(CH_3)_2CH{=}CH_2]C_6H_4\text{-}p\text{-}CH_3$ was obtained in addition to *N*-methyl compound **13**. Related chemistry of anions of the type $(CO)_5W{=}C(R)NRCH_2^-$ will be described in a separate paper.

The crystal was disordered due to some substitution (30%) of a molecule A (with a structure similar to molecule 2) for molecule 1 and substitution (30%) of a molecule B (with a structure similar to molecule 1) for molecule 2. Most of the atoms of molecules A and 2 and of molecules B and 1 about each tungsten atom overlap closely, and no attempts were made to resolve them. Only the $CH_2{=}CHC(CH_3)_2$ fragments and tolyl CH_3 groups of the minor conformations A and B were included in the model, and they are labeled A and B, respectively, in Tables I and II. Inclusion of these atoms of the minor conformations A and B led to chemically more reasonable bond lengths and angles for the atoms of molecules 1 and 2. The minor conformation of molecule 1 was very similar to the major conformation of molecule 2 and vice versa.

We have previously discussed the structure of metal–carbene–alkene complexes in terms of three angles that fully define the relationship between these two ligands. α is the angle between the carbene carbon, the metal, and the midpoint of the alkene C=C bond; for a cis complex $\alpha = 90°$ and for a trans complex $\alpha = 180°$. For (allylamino)carbene complex **3**, the small size of the chelate ring caused a constriction of α to 76.8°. In the present (butenylamino)carbene complex **6**, the larger chelate size allows a relaxation of α to 92.1° and 90.7° for the perpendicular and parallel conformations of **6**. The angle β between the plane defined by the carbene carbon, the metal, and the midpoint of the alkene ligand and plane defined by the metal and the two carbons of the alkene unit determines whether the carbon–carbon double bond of the alkene and the carbene carbon-to-metal bond are parallel ($\beta = 0°$) or perpendicular ($\beta = 90°$). For molecule 1 of butenylamino complex **6**, β is 64.2° and the ligands are closer to a perpendicular arrangement than a parallel one. For molecule 2, β is 3.5° and the ligands are in a nearly parallel arrangement. The angle γ defines the twist between the plane of the carbene carbon, the metal, and the alkene midpoint and the mean plane of the carbene ligand [M=C(R)R′]. For the perpendicular conformation of **6** γ is 44.7°, and for the parallel conformation γ is 42.0°. Molecular models suggest that these twists are mainly due to the conformational requirements of the chelate ring.

The alkene carbon atoms of both conformations of **6** are bonded symmetrically to tungsten. The C5–W and C6–W bond lengths differ by less than 0.01 Å in the perpendicular conformation and by about 0.02 Å for the parallel conformation. The average plane of the tolyl ring is nearly orthogonal to the plane of the carbene ligand in both the perpendicular (85.5°) and parallel (92.7°) conformations of **6**. Consequently, both the ortho and the meta protons are nonequivalent in **6**. Slow rotation of the *p*-tolyl groups allows this nonequivalence to be seen by NMR.

For a cis metal–carbene–alkene complex ($\alpha = 90°$), four extreme geometries are possible, I–IV. Only conformation II ($\beta = 0°$, $\gamma = 90°$) is set up for a smooth conversion to a metallacyclobutane. The alkene and carbene ligands of the parallel conformation of **6** are almost aligned for metallacyclobutane formation; only an increase in γ from 42° to 90° is required for formation of the bicyclo[3.2.0] metallacycle. Examination of molecular models indicates that is easily accomplished. NMR studies to be described below and examination of molecular models both indicate that interconversion of perpendicular and parallel conformations of **6** is very facile.

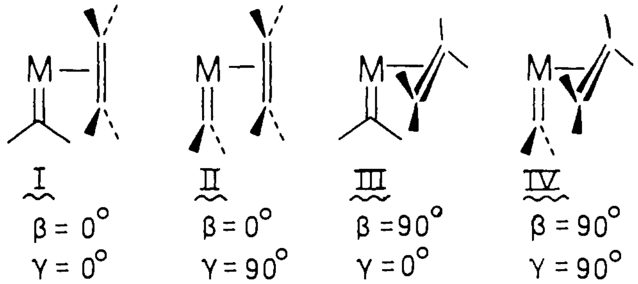

Conformational Equilibrium of Tungsten–Carbene–Alkene Complex 6. Three separate fluxional processes are seen for **6**. First, the parallel and perpendicular conformations of **6** equilibrate rapidly on the NMR time scale at room temperature without alkene decomplexation. Second, there is hindered rotation ($\Delta G^{\ddagger} = 17.0$ kcal mol^{-1}) of the *p*-tolyl ring about the plane of the carbene ligand that becomes rapid on the NMR time scale at 75 °C. Third, decomplexation of the alkene ligand occurs rapidly on the NMR time scale at a slightly higher temperature ($\Delta G^{\ddagger} = 18.8$ kcal mol^{-1}).

The IR spectrum of **6** has six absorptions in the carbonyl region at 2019 (s), 1932 (s), 1924 (s), 1913 (s), 1898 (sh), and 1983 (vs) cm^{-1} instead of only four as expected for a cis-disubstituted tetracarbonyl complex. The extra bands observed for **5** are attributed to the presence of the parallel and perpendicular conformations of **6** observed by X-ray crystallography. These two conformations must be equilibrating rapidly on the NMR time scale at room temperature since no doubling of resonances was seen either in the ^{1}H or ^{13}C NMR spectra of **6**.[19]

The three alkene protons of **6** experience large upfield shifts upon complexation to tungsten and appear as an ABX pattern at δ 3.47 ($J_{cis} = 9.4$ Hz, $J_{trans} = 14.1$ Hz), 3.41 ($J_{cis} = 9.4$ Hz, $J_{gem} = 0.5$ Hz), and 3.14 ($J_{trans} = 14.1$ Hz, $J_{gem} = 0.5$ Hz). In the coupled ^{13}C NMR, the alkene carbons are shifted far upfield and appear at δ 85.5 (d, $J = 158$ Hz) and 56.2 (t, $J = 154$ Hz). Due to the chelate ring, the NCH_2 protons of **6** are diastereotopic and give rise to an AB quartet at δ 3.10 and 2.85 ($J = 13.0$ Hz), and the geminal methyl groups are nonequivalent and appear as two singlets at δ 0.83 and 0.51.

Four distinct resonances are seen for the four protons of the *p*-tolyl group due to hindered rotation about the bond to the carbene carbon. At 6.8 °C, the two upfield signals are well separated and appear as doublets of doublets at δ 6.60 ($J_{ortho} = 8.8$ Hz, $J_{meta} = 2.2$ Hz) and 6.51 ($J_{ortho} = 8.8$ Hz, $J_{meta} = 2.2$ Hz). The observation of splitting by meta coupling is in agreement with an ABXY pattern and is inconsistent with these signals being the upfield portions of AB quartets of two different species present in a 1:1 ratio. The downfield portions of the ABXY pattern appear as a pseudotriplet at δ 7.00 due to two overlapping doublets. This ABXY spectrum is temperature dependent and reaches a limiting spectrum consisting of a single AA′XX′ quartet at 75 °C. Due to smaller differences in chemical shifts, the pseudotriplet at δ 7.00 broadens more rapidly than the higher field doublets of doublets and coalesces at 42 °C. The higher field doublets of doublets at δ 6.6 and 6.5 coalesce at 51 °C.

Selective decoupling of the pseudotriplet at δ 7.0 caused the upfield resonances at δ 6.6 and 6.5 to collapse to singlets. The temperature dependence of this decoupled spectrum was studied since it greatly simplified line-shape analysis of the coalescence of the two singlets. Comparison of the experimental and calculated line shapes over temperatures from 40 to 66 °C gave $\Delta G^{\ddagger} = 17.0$ kcal mol^{-1}.[20] Two different processes could lead to exchange of the environment of the *p*-tolyl protons: first, rotation of the tolyl group about its bond to the carbene carbon atom would interconvert the nonequivalent ortho hydrogens; second, decomplexation of the coordinated alkene and recomplexation to the opposite alkene face would interconvert the environments of the nonequivalent ortho hydrogens without requiring *p*-tolyl rotation. Since we have independently determined (see below) that alkene decomplexation is slower than exchange of the tolyl environment, tolyl rotation is the process involved.

We had not observed hindered aryl rotation for either the oxygen-substituted metal–carbene–alkene complex **1** or the (allylamino)carbene–tungsten complex **3**. One obvious difference between **6** and these complexes is the presence of an $N{-}CH_3$ group which would hinder tolyl rotation. To determine the effect of an $N{-}CH_3$ group on tolyl rotation, we prepared the $N{-}CH_3$ (allylamino)carbene complex **14** and compared it with the N–H

---

[19] No doubling in the ^{1}H NMR of **6** was seen down to −35 °C, but in the ^{13}C NMR at −71 °C selective broadening of the resonance at δ 85.4 due to $CH{=}CH_2$ was observed.

[20] For **6** tolyl resonances, T (°C), k (s^{-1}), $\Delta G^{\ddagger}$ (kcal mol^{-1}): 40.1, 11.0, 16.9; 51.9, 21.5, 17.0; 54.6, 26.0, 17.0; 57.8, 34.0, 17.0; 65.8, 45.0, 17.3.

Table I. Interatomic Distances (Å) for **6**[a]

1W–1C(1)	2.03 (1)	1W–1C(2)	2.01 (1)	2W–2C(1)	1.98 (1)	2W–2C(2)	2.0 (1)
1W–1C(3)	1.97 (1)	1W–1C(4)	1.98 (1)	2W–2C(3)	1.94 (1)	2W–2C(4)	1.98 (1)
1W–1C(5)	2.49 (1)	1W–1C(6)	2.48 (1)	2W–2C(5)	2.42 (1)	2W–2C(6)	2.44 (1)
1W–1C(9)	2.203 (8)	1C(1)–1O(1)	1.16 (1)	2W–2C(9)	2.178 (9)	2C(1)–2O(1)	1.20 (1)
1C(2)–1O(2)	1.16 (1)	1C(3)–1O(3)	1.17 (1)	2C(2)–2O(2)	1.16 (1)	2C(3)–2O(3)	1.21 (1)
1C(4)–1O(4)	1.19 (1)	1C(5)–1C(6)	1.36 (1)	2C(4)–2O(4)	1.17 (1)	2C(5)–2C(6)	1.33 (1)
1C(6)–1C(7)	1.56 (2)	1C(7)–1C(8)	1.51 (2)	2C(6)–2C(7)	1.49 (2)	2C(7)–2C(8)	1.53 (2)
1C(7)–1C(10)	1.56 (2)	1C(7)–1C(11)	1.53 (2)	2C(7)–2C(10)	1.54 (2)	2C(7)–2C(11)	1.59 (2)
1C(8)–1N	1.49 (1)	1N–1C(9)	1.33 (1)	2C(8)–2N	1.49 (1)	2N–2C(9)	1.34 (1)
1N–1C(12)	1.48 (1)	1C(9)–1C(13)	1.48 (1)	2N–2C(12)	1.49 (1)	2C(9)–2C(13)	1.48 (1)
1C(13)–1C(14)	1.40 (1)	1C(14)–1C(15)	1.39 (1)	2C(13)–2C(14)	1.41 (1)	2C(14)–2C(15)	1.41 (1)
1C(15)–1C(16)	1.42 (1)	1C(16)–1C(17)	1.36 (1)	2C(15)–2C(16)	1.43 (2)	2C(16)–2C(17)	1.34 (2)
1C(16)–1C(19)	1.48 (2)	1C(17)–1C(18)	1.38 (1)	2C(16)–2C(19)	1.51 (2)	2C(17)–2C(18)	1.44 (2)
1C(18)–1C(13)	1.44 (1)	1C(16)–AC(19)	1.67 (3)	2C(18)–2C(13)	1.40 (1)	2C(16)–BC(19)	1.72 (4)
1W–AC(5)	2.43 (3)	1W–AC(6)	2.51 (2)	2W–BC(5)	2.49 (2)	2W–BC(6)	2.50 (2)
AC(5)–AC(6)	1.31 (2)	AC(6)–AC(7)	1.64 (7)	BC(5)–BC(6)	1.36 (5)	BC(6)–BC(7)	1.63 (6)
AC(7)–AC(10)	1.72 (7)	AC(7)–AC(11)	1.42 (7)	BC(7)–BC(10)	1.46 (4)	BC(7)–BC(11)	1.55 (5)

[a] The estimated standard deviations of the least significant digits are given in parentheses.

(allylamino)carbene complex **3**. At ambient temperature, the N–CH_3 allylamino complex **14** is undergoing rapid tolyl rotation and a single AB quartet is seen in the aromatic region of its ^1H NMR spectrum. At –65 °C, tolyl rotation is completely frozen out and three broad resonances in a 2:1:1 ratio are seen. Decoupling of the more intense downfield resonance collapsed the upfield resonances and led to determination of a $\Delta G^{\ddagger} = 11.5$ kcal mol^{-1} barrier to tolyl rotation.[21] For the N–H (allylamino)carbene complex **3**, we were unable to detect any barrier to rotation of the tolyl group by low-temperature ^1H NMR spectroscopy. Clearly, the presence of an N–CH_3 group contributes substantially to the tolyl rotation barrier of **6** and **14**. The smaller tolyl rotation barrier of the allylamino complex **14** is probably related to the small angle ($\alpha = 76.8°$) between the carbene and alkene ligands of **14**; this would lead to reduced interaction with carbonyl groups on tungsten during tolyl rotation.

During studies of the tolyl rotation of **6**, an additional fluxional process was discovered that leads to coalescence of the signals due to its diastereotopic geminal methyl groups at 115 °C. Exchange of the chemical environments of the geminal methyl groups requires that the tungsten–alkene bond be severed and that the other face of the alkene form a new bond to tungsten. Computer simulation of the line broadening and coalescence of the geminal dimethyl signals of **5** led to the determination of $\Delta G^{\ddagger} = 18.8$ kcal mol^{-1} for geminal methyl exchange.[22] This alkene dissociation and recomplexation also exchange the environments of the ortho tolyl protons of **6**. However, the significantly higher rates of exchange of tolyl protons ($\Delta G^{\ddagger} = 17.0$ kcal mol^{-1}) indicates that two different processes are responsible for the coalescence of the tolyl resonances and of the geminal methyl resonances.

The relatively high lability of the coordinated alkene in **6** is attributed to a combination of the steric bulk of the alkene ligand (which has geminal methyl substituents on the α carbon atom) and of the unfavorable size of the chelate ring. The less bulky coordinated alkene of (allylamino)carbene complex **3** is in a smaller, more stable chelate ring; no NMR evidence for its decomplexation was obtained.

Alkene Substitution Reactions of 5. The coalescence of the NMR signals of geminal methyl groups of **6** at high temperature was interpreted as arising from alkene dissociation and suggested that the proposed 5-coordinate intermediate might be readily trapped by added ligands. Indeed, **6** reacts rapidly at room temperature with CO, PMe_3, and PPh_3 to form 1:1 adducts in which the alkene ligand is displaced by the incoming nucleophile. The incoming ligand was shown to be cis to the carbene ligand by IR spectroscopy. In all cases, the *Z* isomer about the carbene carbon–nitrogen partial double bond was the kinetically formed product. Subsequent isomerization gave mixtures of *Z* and *E* isomers.

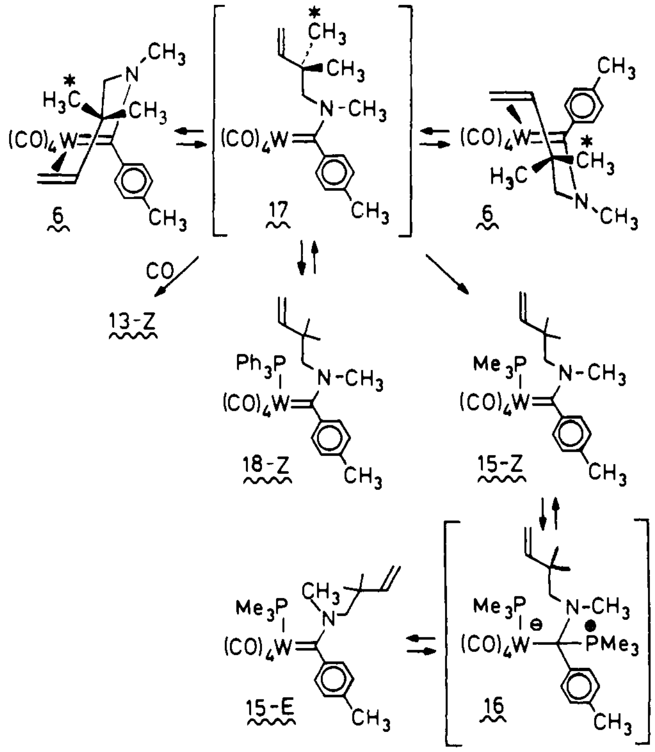

When a solution of **6** in benzene-d_6 was sealed in an NMR tube under 2.8 atm of CO, quantitative replacement of the alkene by CO took place at room temperature over several hours and pure **13**-*Z* was isolated in 78% yield.

Trimethylphosphine reacted rapidly with **6** at room temperature to displace the alkene ligand and produce **15**-*Z* in 78% isolated yield. The formation of **15**-*Z* from **6** and PMe_3 in benzene at 24.9 °C was followed by UV spectroscopy at 425 nm (for **6**, $\epsilon = 388$ M^{-1} cm^{-1}; for **15**-*Z*, $\epsilon = 1150$ M^{-1} cm^{-1}). The observed first-order rate constants for formation of **15**-*Z* increased only slightly from 4.57×10^{-2} to 5.77×10^{-2} s^{-1} when the concentration of PMe_3 was increased from 0.47 to 2.35 M,[23] and the rate constant extrapolated to zero [PMe_3] is 4.2×10^{-2} s^{-1}. The fact that the rate is independent of PMe_3 concentration is consistent with rate-determining dissociation of the alkene ligand. Moreover, when the rates of alkene dissociation measured by reaction with PMe_3 at 24.9 °C and by NMR (twice the rate of geminal methyl ex-

---

(21) For **14**, *T* (°C), *k* (s^{-1}), $\Delta G^{\ddagger}$ (kcal mol^{-1}): –55.4, 33, 11.0; –43.4, 85, 11.3; –32.1, 180, 11.5; –15.5, 1000, 11.4.

(22) For **6** geminal methyls, *T* (°C), *k* (s^{-1}), $\Delta G^{\ddagger}$ (kcal mol^{-1}): 115, 180, 18.8; 102, 70, 18.9; 90, 30, 18.8; 78.8, 16, 18.7; 59, 2.5, 18.8.

(23) First-order rate constants for formation of **15**-*Z* from **6** at 24.9 °C (*k*, [PMe_3]): 4.47 (3) × 10^{-2} s^{-1}, 0.47 M; 4.85 (2) × 10^{-2} s^{-1}, 0.94 M; 5.23 (4) × 10^{-2} s^{-1}, 1.14 M; 5.77 (4) × 10^{-2} s^{-1}, 2.35 M.

Table II. Interatomic Angles (deg) for **6**

1C(1)–1W–1C(2)	170.3 (4)	1C(1)–1W–1C(3)	86.1 (5)
1C(1)–1W–1C(4)	87.2 (4)	1C(1)–1W–1C(5)	110.1 (5)
1C(1)–1W–1C(6)	82.0 (4)	1C(1)–1W–1C(9)	90.8 (3)
1C(2)–1W–1C(3)	84.2 (5)	1C(2)–1W–1C(4)	92.8 (4)
1C(2)–1W–1C(5)	79.5 (4)	1C(2)–1W–1C(6)	107.7 (4)
1C(2)–1W–1C(9)	89.2 (3)	1C(3)–1W–1C(4)	88.8 (4)
1C(3)–1W–1C(5)	160.3 (4)	1C(3)–1W–1C(6)	167.5 (4)
1C(3)–1W–1C(9)	91.4 (3)	1C(4)–1W–1C(5)	81.2 (4)
1C(4)–1W–1C(6)	94.3 (4)	1C(4)–1W–1C(9)	177.9 (4)
1C(5)–1W–1C(6)	31.8 (3)	1C(5)–1W–1C(9)	99.2 (4)
1C(6)–1W–1C(9)	85.0 (3)	1W–1C(1)–1O(1)	174.6 (9)
1W–1C(2)–1O(2)	177.1 (8)	1W–1C(3)–1O(3)	175.4 (9)
1W–1C(4)–1O(4)	177.6 (1.1)	1W–1C(5)–1C(6)	73.7 (6)
1W–1C(6)–1C(5)	74.5 (6)	1W–1C(6)–1C(7)	113.4 (7)
1C(5)–1C(6)–1C(7)	124.0 (1.1)	1C(6)–1C(7)–1C(8)	111.9 (1.1)
1C(6)–1C(7)–1C(10)	103.6 (1.0)	1C(6)–1C(7)–1C(11)	119.7 (1.2)
1C(8)–1C(7)–1C(10)	101.3 (1.0)	1C(8)–1C(7)–1C(11)	107.8 (1.1)
1C(10)–1C(7)–1C(11)	110.9 (1.2)	1C(7)–1C(8)–1N	112.7 (7)
1C(8)–1N–1C(9)	120.0 (7)	1C(8)–1N–1C(12)	114.3 (7)
1C(9)–1N–1C(12)	125.7 (7)	1W–1C(9)–1N	128.4 (6)
1W–1C(9)–1C(13)	117.4 (5)	1N–1C(9)–1C(13)	114.3 (7)
1C(9)–1C(13)–1C(14)	122.5 (7)	1C(9)–1C(13)–1C(18)	119.8 (8)
1C(14)–1C(13)–1C(18)	117.6 (8)	1C(13)–1C(14)–1C(15)	121.4 (8)
1C(14)–1C(15)–1C(16)	120.4 (9)	1C(15)–1C(16)–1C(17)	118.0 (9)
1C(15)–1C(16)–1C(19)	123.6 (1.0)	1C(17)–1C(16)–1C(19)	118.3 (1.0)
1C(16)–1C(17)–1C(18)	123.2 (8)	1C(17)–1C(18)–1C(13)	119.3 (9)
2C(1)–2W–2C(2)	175.3 (4)	2C(2)–2W–2C(3)	87.2 (4)
2C(2)–2W–2C(4)	89.2 (5)	2C(2)–2W–2C(5)	89.8 (5)
2C(2)–2W–2C(6)	91.1 (5)	2C(2)–2W–2C(9)	89.0 (4)
2C(1)–2W–2C(3)	90.4 (4)	2C(1)–2W–2C(4)	86.7 (4)
2C(1)–2W–2C(5)	91.6 (5)	2C(1)–2W–2C(6)	92.4 (5)
2C(1)–2W–2C(9)	94.9 (3)	2C(3)–2W–2C(4)	87.7 (4)
2C(3)–2W–2C(5)	165.1 (5)	2C(3)–2W–2C(6)	162.8 (4)
2C(3)–2W–2C(9)	87.9 (3)	2C(4)–2W–2C(5)	77.6 (5)
2C(4)–2W–2C(6)	109.3 (5)	2C(4)–2W–2C(9)	175.4 (4)
2C(5)–2W–2C(6)	31.7 (4)	2C(5)–2W–2C(9)	106.6 (5)
2C(6)–2W–2C(9)	75.0 (5)	2W–2C(1)–2O(1)	176.4 (9)
2W–2C(2)–2O(2)	178.9 (1.0)	2W–2C(3)–2O(3)	178.5 (8)
2W–2C(4)–2O(4)	175.8 (1.1)	2W–2C(5)–2C(6)	75.0 (8)
2W–2C(6)–2C(5)	73.3 (8)	2W–2C(6)–2C(7)	115.7 (1.0)
2C(5)–2C(6)–2C(7)	133.2 (1.8)	2C(6)–2C(7)–2C(8)	118.4 (1.0)
2C(6)–2C(7)–2C(10)	113.5 (1.6)	2C(6)–2C(7)–2C(11)	105.5 (1.7)
2C(8)–2C(7)–2C(10)	103.0 (1.6)	2C(8)–2C(7)–2C(11)	106.9 (1.4)
2C(10)–2C(7)–2C(11)	109.1 (1.2)	2C(7)–2C(8)–2N	112.0 (9)
2C(8)–2N–2C(9)	119.6 (7)	2C(8)–2N–2C(12)	112.7 (8)
2C(9)–2N–2C(12)	127.6 (8)	2W–2C(9)–2N	127.8 (6)
2N–2C(9)–2C(13)	110.8 (7)	2W–2C(9)–2C(13)	121.3 (6)
2C(9)–2C(13)–2C(14)	120.9 (9)	2C(9)–2C(13)–2C(18)	120.6 (9)
2C(14)–2C(13)–2C(18)	118.5 (9)	2C(13)–2C(14)–2C(15)	122.2 (1.4)
2C(14)–2C(15)–2C(16)	117.6 (1.3)	2C(15)–2C(16)–2C(17)	120.3 (9)
2C(15)–2C(16)–2C(19)	117.1 (1.6)	2C(17)–2C(16)–2C(19)	122.5 (1.7)
2C(16)–2C(17)–2C(18)	122.3 (1.3)	2C(17)–2C(18)–2C(13)	118.9 (1.2)
1C(1)–1W–AC(5)	83.8 (1.0)	1C(1)–1W–AC(6)	100.5 (8)
1C(2)–1W–AC(5)	105.8 (1.0)	1C(2)–1W–AC(6)	88.8 (8)
1C(3)–1W–AC(5)	166.4 (9)	1C(3)–1W–AC(6)	162.2 (7)
1C(4)–1W–AC(5)	81.6 (9)	1C(4)–1W–AC(6)	107.9 (7)
1C(9)–1W–AC(5)	97.8 (9)	1C(9)–1W–AC(6)	72.0 (7)
AC(5)–1W–AC(6)	30.7 (6)	1W–AC(5)–AC(6)	77.9 (1.6)
1W–AC(6)–AC(5)	71.5 (1.6)	1W–AC(6)–AC(7)	119.6 (3.1)
AC(5)–AC(6)–AC(7)	93.8 (3.6)	AC(6)–AC(7)–AC(10)	102.0 (4.7)
AC(6)–AC(7)–AC(11)	121.0 (5.5)	AC(19)–1C(16)–1C(15)	113.7 (1.3)
AC(19)–1C(16)–1C(17)	127.7 (1.2)	2C(1)–2W–BC(5)	105.6 (6)
2C(1)–2W–BC(6)	76.3 (5)	2C(2)–2W–BC(5)	76.5 (6)
2C(2)–2W–BC(6)	106.5 (5)	2C(3)–2W–BC(5)	163.0 (6)
2C(3)–2W–BC(6)	165.2 (5)	2C(4)–2W–BC(5)	87.4 (7)
2C(4)–2W–BC(6)	97.9 (6)	2C(9)–2W–BC(5)	96.3 (7)
2C(9)–2W–BC(6)	86.7 (5)	BC(5)–2W–BC(6)	31.7 (4)
2W–BC(5)–BC(6)	74.5 (1.0)	2W–BC(6)–BC(5)	73.8 (1.1)
2W–BC(6)–BC(7)	118.7 (2.0)	BC(5)–BC(6)–BC(7)	126.0 (3.0)
BC(6)–BC(7)–BC(10)	112.3 (3.6)	BC(6)–BC(7)–BC(11)	103.0 (4.2)
BC(10)–BC(7)–BC(11)	113.6 (3.5)	BC(19)–2C(16)–2C(15)	128.7 (4.0)

change) at higher temperatures were plotted on the same ln (k/T) vs. $1/T$ plot a good straight line ($R = 0.9941$) was obtained and values of $\Delta H^{\ddagger} = 21.9 \pm 1.2$ kcal mol^{-1} and $\Delta S^{\ddagger} = 9.4 \pm 3.4$ eu mol^{-1} were calculated.

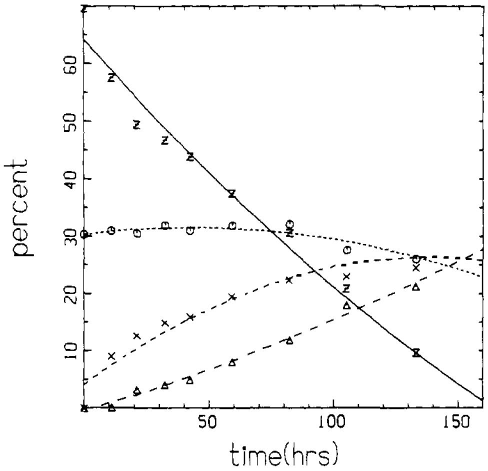

Figure 3. Thermolysis of **13** (0.26 M in benzene-d_6) at 98.6 °C followed by ^1H NMR. (Z) **13**-*Z*; (⊙) **13**-*E*; (X) **6**; (△) **7**. Percents are based on integration of the geminal methyl signals and comparison with the integration of the methyl signal of the internal standard *p*-bis(trimethylsilyl)benzene.

When the *Z*-isomer of PMe_3 adduct **15**-*Z* was heated at 88 °C for 1 h, isomerization to a 1:1 mixture of **15**-*Z* and **15**-*E* occurred. The rate of this isomerization is substantially faster than the isomerization of **6**. This rapid isomerization can be explained by reversible nucleophilic attack of PMe_3 at the carbene carbon atom of **15**-*Z* which would generate an intermediate (**16**) without a configuration holding π-bond between nitrogen and the carbene carbon.

Evidence that small concentrations of PMe_3 are available to catalyze the *Z* to *E* isomerization comes from the observation that heating a 1.3:1 mixture of **15**-*Z* and N-CD_3-labeled **6** at 88 °C for 3 h gave a 2:1:1 ratio of **6**:**15**-*Z*:**15**-*E* in which scrambling of N-CH_3 and N-CD_3 had occurred.[24] This scrambling process undoubtedly occurs via common intermediate **17** formed by loss of PMe_3 from **15** and by alkene dissociation from **6**.

Reaction of **6** (0.07 M) with PPh_3 (0.15 M) in benzene-d_6 at room temperature led to the rapid formation of a 95:5 mixture of PPh_3 substitution product **18**-*Z* and starting material **6**. **18**-*Z* was readily characterized by ^1H NMR spectroscopy,[25] but attempted isolation of pure material was always frustrated by partial dissociation of PPh_3 and re-formation of some contaminating starting material **6**.

The equilibrium constant for formation of **18**-*Z* from PPh_3 and **6** was determined by NMR to be $K_{eq} = 137 \pm 3\ M^{-1}$ at 22 °C.[26] At 88.5 °C, the carbene-phosphine complex is less strongly favored and $K_{eq} = 13.7 \pm 1.5\ M^{-1}$.[27] At the higher temperature, isomerization also produced **18**-*E*.[28]

Thermal Cyclopropane Formation. The thermolysis of a 2.3:1 mixture of **13**-*Z* and **13**-*E* in benzene-d_6 at 98.6 °C was followed by NMR, and the major species formed as a function of time are shown in Figure 3. **13**-*Z* was converted to metal-carbene-alkene complex **6** and cyclopropane **7** much more rapidly than **13**-*E*. This caused the *Z*:*E* ratio to decrease to 1:1 after 82 h. The observation of different Z:E ratios at different times indicates that *Z* to *E* isomerization is slow relative to conversion of *Z* to other products. The more rapid disappearance of **13**-*Z* establishes that it is the direct precursor of tungsten-carbene-alkene complex **6** and confirms its *Z* stereochemistry. The amount of **13**-*E* present remains approximately constant until most of **13**-*Z* has reacted and then decreases slowly. This can be explained in terms of slow *E* to *Z* isomerization and draining off of **13**-*Z* to other products.

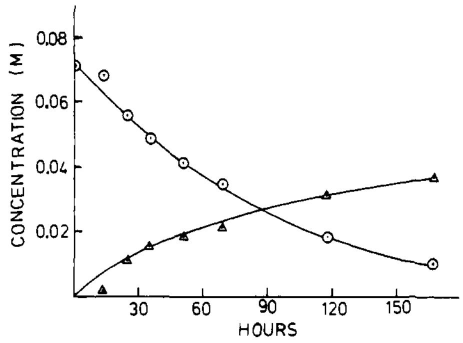

Figure 4. Thermolysis of **6** (0.071 M in benzene-d_6) at 88.0 °C followed by NMR: (⊙) **6**; (△) **7** + **19**.

Cyclopropane **7** appeared only after an appreciable amount of carbene-alkene complex **6** had formed. This is consistent with the formation of **7** from **6** and not directly from either **13**-*Z* or **13**-*E*. The amount of **6** levels off after about 100 h and then decreases while the amount of cyclopropane **7** rises continuously. The rates of conversion of **13**-*Z* to **6** and of **6** to **7** are apparently quite similar. The best isolated yields of tungsten-carbene-alkene complex **6** are therefore obtained after about 75 h at 98.6 °C.

The isolated tungsten-carbene-alkene complex **6** is also converted to cyclopropane **7** on thermolysis at 88 °C in benzene-d_6 (Figure 4). A smooth first-order disappearance of **6** was seen. After an appreciable amount of cyclopropane **7** was observed, another minor product began to appear and was identified by ^1H NMR as the tricarbonyltungsten arene complex of **6**, **19**.[29]

The most straightforward mechanism for cyclopropane formation from tungsten-carbene-alkene complex **6** involves formation of metallacycle **20** and reductive elimination; we believe that this is the operative mechanism. However, the fact that the alkene ligand of **6** is undergoing reversible decomplexation much more rapidly than cyclopropane formation makes it impossible to exclude mechanisms involving reaction of the tungsten-carbene unit with an uncomplexed alkene. Attack on uncomplexed alkenes occurs in the cyclopropane-forming reaction of highly electrophilic carbene complexes such as $(CO)_5W = CHC_6H_5$[30] and $C_5H_5(CO)_2Fe{=}C(CH_3)_2^+$.[31]

Photochemical Cyclopropane Formation. Photolysis of a 1:13 mixture of **13**-*Z*:**13**-*E*[32] in THF-d_8 (0.16 M) with 350-mn light at 35 °C was followed by ^1H NMR spectroscopy. As in the case of other aminocarbene complexes,[13] the most rapid photochemical reaction was *E* to *Z* isomerization that led to formation of a 1.3:1 **13**-*Z*:**13**-*E* photostationary state. In addition, photochemical extrusion of CO led to formation of tungsten-carbene-alkene complex **6**, and on extended photolysis **6** was converted to cy-

---

[24] NMR showed that 56% of **6** contained N-CH_3 groups and 51% of **15**-*Z* contained N-CH_3 groups. Overlap with alkene resonances of **6** prevented analysis of the N-CH_3 groups of **15**-*E*.

[25] ^1H NMR of **18-Z** (270 MHz, C_6D_6): δ 7.60 (m, 6 H), 6.98 (m, not integrated due to free PPh_3 resonance), 6.85 (d, J = 7.35 Hz), 6.34 (d, J = 7.35 Hz), 5.68 (dd, J = 17.5, 10.8 Hz, 1 H, $CH{=}CH_2$), 4.80 (d, J = 10.8 Hz, 1 H, $CH{=}CHH$), 4.77 (d, J = 17.4 Hz, 1 H, $CH{=}CHH$), 3.66 (br s, 2 H, NCH_2), 2.35 (s, 3 H, NCH_3), 2.04 (s, 3 H, $ArCH_3$), 1.08 (s, 6 H, $C(CH_3)_2$).

[26] At 22 °C [**6**], [PPh_3], [**18**-*Z*], K_{eq}: 0.024, 0.010, 0.03, 140 M^{-1}; 0.011, 0.020, 0.053, 139 M^{-1}; 0.017, 0.023, 0.055, 138 M^{-1}; 0.0067, 0.045, 0.041, 133 M^{-1}.

[27] At 88.5 °C, [**6**], [PPh_3], [**18**-*Z*], K_{eq}: 0.040, 0.043, 0.027, 15.3 M^{-1}; 0.043, 0.043, 0.022, 11.9 M^{-1}; 0.022, 0.17, 0.048, 13.1 M^{-1}; 0.010, 0.18, 0.025, 14.1 M^{-1}.

[28] ^1H NMR of **18**-*E* (270 MHz, C_6D_6): δ 7.46 (m, 6 H), 6.98 (m, not integrated due to overlap with **18**-*Z* and PPh_3), 6.78 (d, J = 8.40 Hz, 2 H), 5.38 (dd, J = 16.6, 11.3 Hz, 1 H, $CH{=}CH_2$), about 4.8 (not resolved due to overlap with **18**-*Z*, 2 H, $CH{=}CH_2$), 3.46 (s, 3 H, NCH_3), 2.97 (br s, 2 H, NCH_2), 2.05 (s, 3 H, Ar-CH_3), 0.59 (s, 6 H, $C(CH_3)_2$).

[29] While **19** was not obtained as a pure compound, preparative TLC (hexane-CH_2Cl_2-EtOH 1:1:1) gave a small amount of material which was a 3:1 mixture of **7** and **19**. This mixture allowed all but one of the ^1H NMR resonances of **19** to be assigned. ^1H NMR (270 MHz, C_6D_6): δ 2.43 (d, J = 9.19 Hz, 1 H, NCHH), 1.97 (s, 3 H, NCH_3), 1.72 (s, 3 H, $ArCH_3$), 1.44 (d, J = 9.19 Hz, 1 H, NCHH), 1.12 (s, 3 H, $C(CH_3)CH_3$), 0.87 (s, 3 H, $C(CH_3)CH_3$), 0.67 (dd, J = 8.3, 4.6 Hz, 1 H, cyclopropyl CH), 0.43 (dd, J = 8.2, 6.1 Hz, 1 H, cyclopropyl CH_2, exo), not observed (cyclopropyl CH_2, endo).

[30] Casey, C. P.; Polichnowski, S. W.; Shusterman, A. J.; Jones, C. R. *J. Am. Chem. Soc.* **1979**, *101*, 7282-7292.

[31] Casey, C. P.; Miles, W. M.; Tukada, H.; O'Connor, J. M. *J. Am. Chem. Soc.* **1982**, *104*, 3761-3762.

[32] The highly enriched **10**-*E* was obtained by recovery of **10** from thermolysis reactions.

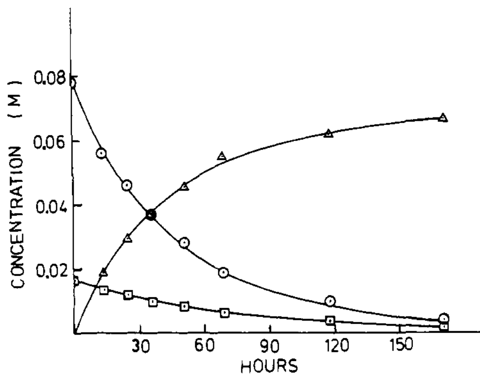

Figure 5. Thermolysis of **6** (0.078 M in benzene-d_6) in the presence of PPh_3 (0.20 M) at 88 °C followed by NMR: (⊙) total tungsten-carbene complexes **6**, **13**-*Z*, and **13**-*E*; (△) **7**; (□) calculated concentration of **6**.

clopropane **7**. After 106 h of irradiation, the reaction mixture consisted of 23% **13**-*Z*, 17% **13**-*E*, 31% **6**, and 18% **7**.

In a separate experiment, photolysis of tungsten–carbene–alkene complex **6** (0.13 M, $\epsilon = 8.16 \times 10^{-3}$ at 350 nm) in THF-d_8 with 350-nm light was followed by ^1H NMR. After 2 weeks the mixture consisted of 27% starting material **6** and 48% cyclopropane **7**. There are several possible mechanisms for photochemical production of the cyclopropane **7** from the carbon–alkene complex **6**, one of which is light-induced formation of metallacyclobutane complex **20** followed by reductive elimination.[33]

Phosphine-Assisted Cyclopropane Formation. Several important differences were noted when tungsten–alkene–carbene complex **6** was heated at 88 °C in the presence of PPh_3. First, yields of cyclopropane climbed to 90%. Second, *trans*-$W(CO)_4(PPh_3)_2$ was the major tungsten-containing product, and none of the tungstentricarbonyl(arene) complex of the cyclopropane (**19**) was observed. Third, the rate of carbene complex decomposition was noticeably faster.

During the course of this pyrolysis, *trans*-$W(CO)_4(PPh_3)_2$ partially precipitated from solution, and after completion of the pyrolysis it was isolated in 44% yield by crystallization. *trans*-$W(CO)_4(PPh_3)_2$ is a known compound[34] and was identified by its infrared band at 1891 cm^{-1} and by its ^1H NMR spectrum in benzene, which consisted of multiplets at δ 7.76, 7.04, and 6.93 in a 2:2:1 ratio.

The qualitatively faster rate of cyclopropane formation in the presence of PPh_3 is surprising since PPh_3 reacts rapidly with **6** in an equilibrium reaction to displace the alkene ligand and form phosphine complexes **18**-*Z* and **18**-*E* in which the alkene is not coordinated to tungsten. If the only route to cyclopropane involves tungsten–carbene–alkene complex **6**, then PPh_3 should have slowed cyclopropane formation. To clarify the situation, the kinetics of the formation of cyclopropane in the presence of PPh_3 were measured at 88 °C in a kinetic run which paralleled the run in the absence of PPh_3 shown in Figure 4.

A benzene-d_6 solution containing 0.078 M **6** and 0.20 M PPh_3 was heated at 88 °C and periodically monitored at room temperature by ^1H NMR spectroscopy. Figure 5 shows the decrease in total concentration of tungsten–carbene complexes and the increase in cyclopropane concentrations as a function of time. Comparison of Figures 4 and 5 clearly shows the higher rate of disappearance of tungsten–carbene complexes in the presence of PPh_3. When the ^1H NMR of the reaction mixture was run at ambient temperature approximately 1:1 ratios of phosphine complexes **18**-*Z*:**18**-*E* were seen. At 88 °C, the equilibrium mixture also contains significant amounts of tungsten–carbene–alkene complex **6**. The first-order rate constant for disappearance of tungsten–carbene complexes was calculated to be $3.3\ (1) \times 10^{-6}\ s^{-1}$ in the absence of PPh_3 and $4.9\ (1) \times 10^{-6}\ s^{-1}$ in the 0.20 M PPh_3 run.

A more dramatic illustration of the acceleration of cyclopropane formation by PPh_3 can be seen if the rate of formation of cyclopropane is compared with the concentration of tungsten–carbene–alkene complex **6**. The concentration of **6** at various times during the reaction was calculated by using $K_{eq} = [\mathbf{18}\text{-}Z][PPh_3]^{-1}[\mathbf{6}]^{-1} = 13.7\ M^{-1}$ at 88 °,C and $[\mathbf{18}\text{-}Z] = [\mathbf{18}\text{-}E]$ at 88 °C and assuming that equal amounts of cyclopropane **7** and *trans*-$W(CO)_4[P(C_6H_5)_3]_2$ were formed. Even though the concentration of **6** in the presence of PPh_3 is *5 times less* than in the absence of PPh_3 between 20 and 40 h, the rate of disappearance of carbene complexes is *1.5 times greater* in the presence of PPh_3 and cyclopropane formation is *2.5 times greater* in the presence of PPh_3. Clearly, PPh_3 accelerates the conversion of tungsten–carbene complexes to cyclopropane.

One possible explanation for faster formation of cyclopropane **7** in the presence of PPh_3 is that formation of **7** is reversible and that PPh_3 merely traps $W(CO)_4$ and stops the reverse reaction. This possibility was tested by heating a benzene-d_6 solution of NCD_3-labeled **6** in the presence of NCH_3 cyclopropane **7** (4:1 molar ratio). After 165 h at 88 °C, 20% of **6** remained and no NCH_3 resonance due to **6** was observed.

A more likely role for PPh_3 involves a second phosphine-assisted route to cyclopropane. One mechanistically attractive route that involves phosphine assistance involves rate-determining attack of PPh_3 on metallacyclobutane **20**. The 18-electron tungsten–carbene–complex **6** is proposed to be in rapid equilibrium with 16-electron metallacyclobutane **20**; in the absence of PPh_3, the metallacycle could decompose to cyclopropane and a very unstable 14-electron $W(CO)_4$ fragment or revert to **6**. Reaction of PPh_3 with the metallacycle **20** could lead to the 18-electron phosphine-substituted metallacycle **21**, which decomposes rapidly to cyclopropane and a more stable 16-electron $W(CO)_4(PPh_3)$ fragment. The acceleration by phosphine then is the result of trapping of metallacycle **20** and increasing the probability that once generated it will go on to cyclopropane rather than revert to tungsten–carbene–alkene complex **6**. While there are many other routes that could also explain phosphine-assisted cyclopropane formation, the one outlined above is our current favorite.

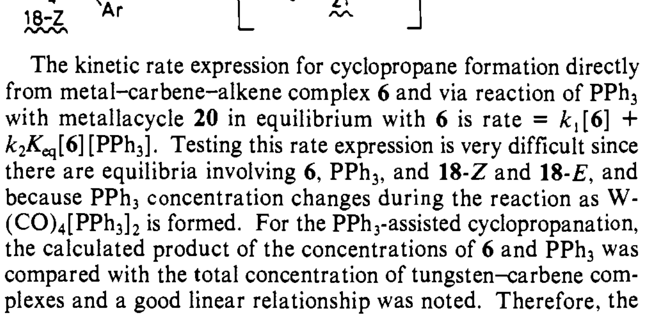

The kinetic rate expression for cyclopropane formation directly from metal–carbene–alkene complex **6** and via reaction of PPh_3 with metallacycle **20** in equilibrium with **6** is rate = $k_1[\mathbf{6}] + k_2K_{eq}[\mathbf{6}][PPh_3]$. Testing this rate expression is very difficult since there are equilibria involving **6**, PPh_3, and **18**-*Z* and **18**-*E*, and because PPh_3 concentration changes during the reaction as $W(CO)_4[PPh_3]_2$ is formed. For the PPh_3-assisted cyclopropanation, the calculated product of the concentrations of **6** and PPh_3 was compared with the total concentration of tungsten–carbene complexes and a good linear relationship was noted. Therefore, the fact that cyclopropanation was first order in total tungsten–carbene concentration is not inconsistent with the above mechanism.

Conclusion

We have succeeded in synthesizing a metal–carbene–alkene complex and shown by X-ray crystallography that conformations

---

[33] The lowest energy excited state of an aminocarbene complex arises from promotion of an electron localized on tungsten to the metal–carbene π^* orbital. Population of this π^* orbital could aid metallacycle formation by decreasing the bond orders between tungsten and the carbene carbon (which occurs in metallacycle formation) and between the carbene carbon and nitrogen (which would increase conformational mobility needed for metallacycle formation).

[34] Magee, T. A.; Matthews, C. N.; Wang, T. S.; Wotiz, J. H. *J. Am. Chem. Soc.* **1961**, *83*, 3200–3203.

in which the carbene and alkene ligands are parallel or perpendicular are both possible. We have found that this metal–carbene–alkene complex (**6**) rapidly and reversibly dissociates its alkene ligand and that it is the precursor of cyclopropane **7**. Curiously, added phosphine assists cyclopropane formation. In future work, we will try to modify the structure of the metal–carbene–alkene complex so that metathesis-like reactions will become favored relative to cyclopropanation.

Experimental Section

General. All reactions were carried out in flame-dried glassware under a nitrogen atmosphere. Benzene, pentane, tetrahydrofuran, and xylene were distilled from purple solutions prepared from sodium and benzophenone immediately prior to use. Hexane and toluene were dried over sodium benzophenone and stored over 4-Å molecular sieves. Dichloromethane ($\mathrm{CH_2Cl_2}$) was purified by preparative thin-layer chromatography (TLC) using Merck silica gel 60 PF-254.

^{1}H NMR spectra were obtained on Bruker WH-270 or Bruker WP-200 spectrometers; when quantitative results were required, a 30-s pulse repetition rate was employed to minimize the effects of different relaxation times. ^{13}C NMR spectra were obtained on a JEOL FX-200 spectrometer; when reported, multiplicities of ^{13}C resonances and the corresponding C–H coupling constants were determined by using an INEPT[35] pulse sequence. The temperatures reported for variable-temperature NMR studies were measured by placement of an NMR tube containing a thermocouple into the NMR probe; 20 min was allowed for temperature equilibration before data acquisition. Simulations of variable-temperature NMR spectra were performed by using a program (NMRSIM) written by M. W. Chen and D. F. Hillenbrand for the Harris/7 computer. Infrared spectra were obtained on a Beckman IR-4230 spectrophotometer. Mass spectra were obtained on an AEI-MS-902 mass spectrometer. Melting points were determined on a Thomas-Hoover capillary melting point apparatus and are uncorrected. UV-visible spectra were measured on a Cary 118 spectrophotometer which for kinetic measurement was equipped with a circulating constant-temperature cuvette holder. Photochemical experiments were carried out in a Rayonet Srinivasan-Griffin photochemical reactor equipped with Sylvania F8T5 bulbs (maximum emission at 350 nm). Constant-temperature thermolysis experiments were carried out in a thermostated bath (±0.2 °C).

2,2-Dimethyl-3-butenenitrile (9). 3-Butenenitrile (0.124 mol, Aldrich) was added to a solution of lithium diisopropylamide (LDA, 0.124 mol) in 300 mL of THF at −78 °C. After 30 min, iodomethane (0.124 mol) was added and the solution was warmed to room temperature. The solution was then cooled to −78 °C and a second equivalent of LDA (0.124 mol in 200 mL THF) was added. After 30 min, iodomethane (0.124 mol) was added. The solution was warmed to room temperature and 250 mL of 1 N $\mathrm{H_2SO_4}$ was added. The aqueous layer was extracted with ether (3 × 100 mL), and the combined ether layers were dried ($\mathrm{MgSO_4}$) and distilled to give **9** (3.86 g, 33%), bp 117 °C. IR (neat): 2238 cm^{-1} ($\mathrm{C{\equiv}N}$). ^{1}H NMR (270 MHz, acetone-d_6): δ 5.85 (dd, J = 17.1, 10.3 Hz, 1 H, $\mathrm{C}\mathit{H}{=}\mathrm{CH_2}$), 5.37 (dd, J = 17.1, 0.5 Hz, 1 H, $\mathrm{CH{=}CH}\mathit{H}$), 5.16 (dd, J = 10.3, 0.5 Hz, 1 H, $\mathrm{CH{=}C}\mathit{H}\mathrm{H}$), 1.41 (s, 6 H). ^{13}C{^{1}H} NMR (50.1 MHz, acetone-d_6): δ 143.6 ($\mathit{C}\mathrm{H{=}CH_2}$), 117.3 ($\mathrm{C{\equiv}N}$), 108.0 ($\mathrm{CH{=}}\mathit{C}\mathrm{H_2}$), 29.8 ($\mathit{C}\mathrm{(CH_3)_2}$), 20.9 ($\mathrm{CH_3}$).

Attempted preparation by treatment of 3-butenenitrile with 2 equiv of $\mathrm{CH_3Li}$ at −100 °C and 2 equiv of $\mathrm{CH_3I}$ at −78 °C[14] led to **9** contaminated with 3,3-dimethyl-1-penten-4-one.

1-Amino-2,2-dimethyl-3-butene (8). A solution of $\mathrm{AlCl_3}$ (5.12 g, 38.4 mmol) in 75 mL of ether was added slowly to $\mathrm{LiAlH_4}$ (1.46 g, 38.4 mmol) suspended in 100 mL of ether. 9 (3.65 g, 38.4 mmol) in 100 mL of ether was added over 1 h. The suspension was stirred for an additional hour, cooled to 0 °C, and quenched by slow addition of 15 mL of $\mathrm{H_2O}$, 70 mL of 6 N $\mathrm{H_2SO_4}$, and 50 mL of $\mathrm{H_2O}$. The aqueous layer was extracted with ether (3 × 100 mL) and cooled to 0 °C. KOH pellets were added until the pH was greater than 7. Precipitated aluminum salts were removed by filtration and the aqueous solution was extracted with ether (3 × 100 mL). The ether extracts were dried ($\mathrm{MgSO_4}$) and distilled to give **8** (1.65 g, 16.7 mmol, 43%), bp 87 °C. IR (neat): 3380 (m, br), 3310 (m, br), 3082 (m), 1639 (m), 1610 (w, br), 1000 (m), 920 (s) cm^{-1}. ^{1}H NMR (270 MHz, $\mathrm{C_6D_6}$): δ 5.60 (dd, J = 17.2, 11.1 Hz, 1 H, $\mathrm{C}\mathit{H}{=}\mathrm{CH_2}$), 4.93 (dd, J = 10.7, 1.5 Hz, 1 H, $\mathrm{CH{=}C}\mathit{H}\mathrm{H}$), 4.88 (dd, J = 17.3, 1.5 Hz, 1 H, $\mathrm{CH{=}CH}\mathit{H}$), 2.31 (s, 2 H, $\mathrm{CH_2}$), 0.84 (s, 6 H, $\mathrm{C(C}\mathit{H}\mathrm{_3)_2}$), 0.63 (br s, 2 H, $\mathrm{NH_2}$). ^{13}C{^{1}H} NMR (50.1 MHz, acetone-d_6): δ 148.4 ($\mathit{C}\mathrm{H{=}CH_2}$), 110.7 ($\mathrm{CH{=}}\mathit{C}\mathrm{H_2}$), 62.6 ($\mathrm{CH_2}$), 38.4 ($\mathit{C}\mathrm{(CH_3)_2}$), 25.4 ($\mathrm{C(}\mathit{C}\mathrm{H_3)_2}$).

Anal. Calcd for $\mathrm{C_6H_{13}N}$: C, 72.73; H, 13.13; N, 14.14. Found: C, 72.45; H, 13.25; N, 14.37.

Pentacarbonyl[((2,2-dimethyl-3-butenyl)amino)(*p*-tolyl)carbene]tungsten(0) (10-*Z* and 10-*E*). Addition of **8** (0.754 g, 7.62 mmol) to a red solution of $\mathrm{(CO)_5WC(OCH_3)C_6H_4\text{-}\mathit{p}\text{-}CH_3}$ (4.19 g, 9.14 mmol) in 600 mL of ether resulted in an orange solution. Column chromatography (silica gel, 9:1 hexane–$\mathrm{CH_2Cl_2}$) yielded three fractions: (A) 200 mL, 1.17 g of $\mathrm{(CO)_5W{=}C(OCH_3)C_6H_4\text{-}\mathit{p}\text{-}CH_3}$; (B) 60 mL, 0.23 g of red oil, mixture of $\mathrm{(CO)_5W{=}C(OCH_3)C_6H_4\text{-}\mathit{p}\text{-}CH_3}$ and **10**; (C) 300 mL, orange oil, mostly **10**. Column chromatography of C (silica gel, toluene) gave **10** as a waxy yellow solid (2.52 g, 63%, 2.9:1 mixture of *Z* and *E* isomers), mp 67–75 °C. IR (cyclohexane): 2063 (m), 1975 (w), 1945 (vs), 1938 (sh) cm^{-1}. NMR spectra of the major and minor isomers were assigned on the basis of relative intensities.

For **10**-*Z*: ^{1}H NMR (270 MHz, THF-d_8) δ 9.54 (br s, 1 H, NH), 7.17 (d, J = 8.3 Hz, 2 H), 6.95 (d, J = 8.5 Hz, 2 H), 5.97 (dd, J = 17.6, 10.5 Hz, 1 H, $\mathrm{C}\mathit{H}{=}\mathrm{CH_2}$), 5.13 (dd, J = 17.6, 1.3 Hz, 1 H, $\mathrm{CH{=}C}\mathit{H}\mathrm{H}$), 5.12 (dd, J = 10.7, 1.1 Hz, 1 H, $\mathrm{CH{=}CH}\mathit{H}$), 3.91 (d, J = 5.9 Hz, 2 H, $\mathrm{NCH_2}$), 2.33 (s, 3 H, $\mathrm{ArC}\mathit{H}\mathrm{_3}$), 1.21 (s, 6 H, $\mathrm{C(C}\mathit{H}\mathrm{_3)_2}$). ^{13}C{^{1}H} NMR (50.1 MHz, $\mathrm{CD_3CN}$, 0.11 M $\mathrm{Cr(acac)_3}$): δ 256.5 (carbene), 205.0 (trans CO), 199.4 (cis CO's), 154.0 (ipso or para), 145.5 ($\mathit{C}\mathrm{H{=}CH_2}$), 139.4 (ipso or para), 129.6, 123.2 (ortho, meta), 114.7 ($\mathrm{CH{=}}\mathit{C}\mathrm{H_2}$), 65.6 ($\mathrm{NCH_2}$), 38.3 ($\mathit{C}\mathrm{(CH_3)_2}$), 25.0 ($\mathrm{C(}\mathit{C}\mathrm{H_3)_2}$), 21.0 ($\mathrm{Ar{-}}\mathit{C}\mathrm{H_3}$).

For **10**-*E*: ^{1}H NMR (270 MHz, THF-d_8): δ, 9.71 (br s, 1 H, $\mathrm{N}\mathit{H}$), 7.21 (d, J = 8.3 Hz, 2 H), 6.79 (d, J = 8.3 Hz, 2 H), 5.75 (dd, J = 17.5, 10.7 Hz, 1 H, $\mathrm{C}\mathit{H}{=}\mathrm{CH_2}$), 5.18 (dd, J = 10.7, 1.1 Hz, 1 H, $\mathrm{CH{=}C}\mathit{H}\mathrm{H}$), 5.17 (dd, J = 17.6, 1.1 Hz, 1 H, $\mathrm{CH{=}CH}\mathit{H}$), 3.14 (d, J = 6.4 Hz, 2 H, $\mathrm{NCH_2}$), 2.34 (s, 3 H, $\mathrm{ArC}\mathit{H}\mathrm{_3}$), 0.98 (s, 6 H, $\mathrm{C(CH_3)_2}$). ^{13}C{^{1}H} NMR (50.1 MHz, $\mathrm{CD_3CN}$, 0.11 M $\mathrm{Cr(acac)_3}$): δ 200.7 (trans CO), 199.5 (cis CO's), 148.9 (ipso or para), 145.3 ($\mathit{C}\mathrm{H{=}CH_2}$), 137.8 (ipso or para), 129.6, 121.8 (ortho, meta), 114.9 ($\mathrm{CH{=}}\mathit{C}\mathrm{H_2}$), 60.0 ($\mathrm{NCH_2}$), 24.5 ($\mathrm{C(}\mathit{C}\mathrm{H_3)_2}$), 21.0 ($\mathrm{Ar}\mathit{C}\mathrm{H_3}$), not observed (carbene, $\mathit{C}\mathrm{(CH_3)_2}$).

***N*-*p*-Tolyl-2,2-dimethyl-3-butenylimine (11).** An authentic sample of **11** was prepared from **8** (20.0 mg, 2.02 mmol) and *p*-tolualdehyde (266 mg, 2.22 mmol) in 15 mL of benzene by azeotropic distillation of water. Vacuum distillation (58–60 °C, 1.5 mmHg) gave imine **11** (90 mg, 22%). IR (neat): 1701 (m), 1648 (s) cm^{-1}. ^{1}H NMR (270 MHz, $\mathrm{C_6D_6}$): δ 7.99 (s, 1 H, $\mathrm{N{=}C(Ar)}\mathit{H}$), 7.70 (d, J = 8.3 Hz, 2 H), 6.97 (d, J = 8.1 Hz, 2 H), 5.99 (dd, J = 17.5, 10.7 Hz, 1 H, $\mathrm{C}\mathit{H}{=}\mathrm{CH_2}$), 5.05 (dd, J = 17.5, 1.5 Hz, 1 H, $\mathrm{CH{=}C}\mathit{H}\mathrm{H}$), 4.99 (dd, J = 10.7, 1.5 Hz, 1 H, $\mathrm{CH{=}CH}\mathit{H}$), 3.36 (d, J = 1.3 Hz, 2 H, $\mathrm{NC}\mathit{H}\mathrm{_2}$), 2.03 (s, 3 H, $\mathrm{ArC}\mathit{H}\mathrm{_3}$), 1.14 (s, 6 H, $\mathrm{C(C}\mathit{H}\mathrm{_3)_2}$).

Pentacarbonyl[((*N*,2,2-trimethyl-3-butenyl)amino)(*p*-tolyl)carbene]tungsten(0) (13-*Z* and 13-*E*). A solution of LDA (2.42 mmol) in 15 mL of THF was added to a solution of **10**-*Z* and **10**-*E* (3.2:1, 1.15 g, 2.20 mmol) in 60 mL of THF at −72 °C. The solution was warmed to room temperature, cooled back to −72 °C, and $\mathrm{CH_3I}$ (2.9 mmol) was added. The solution was stirred for 1 h at room temperature and the THF was evaporated. Column chromatography (silica gel, toluene) gave a 3:1 mixture of **13**-*Z* and **13**-*E* (1.00 g, 85% as yellow oil). IR (cyclohexane): 2055 (m), 1975 (w), 1936 (vs), 1910 (sh) cm^{-1}. NMR spectra of the major and minor isomers were assigned on the basis of relative intensities.

For **13**-*Z*: ^{1}H NMR (270 MHz, $\mathrm{C_6D_6}$): δ 6.89 (d, J = 8.3 Hz, 2 H), 6.52 (d, J = 8.3 Hz, 2 H), 5.65 (dd, J = 17.4, 11.0 Hz, 1 H, $\mathrm{C}\mathit{H}{=}\mathrm{CH_2}$), 4.75 (d, J = 10.8 Hz, 1 H, $\mathrm{CH{=}C}\mathit{H}\mathrm{H}$), 4.67 (d, J = 17.5 Hz, 1 H, $\mathrm{CH{=}CH}\mathit{H}$), 3.88 (s, 2 H, $\mathrm{NCH_2}$), 2.20 (s, 3 H, $\mathrm{NCH_3}$), 2.05 (s, 3 H, $\mathrm{ArCH_3}$), 0.96 (s, 6 H, $\mathrm{C(CH_3)_2}$). ^{13}C{^{1}H} NMR (50.1 MHz, $\mathrm{C_6D_6}$, 0.09 M $\mathrm{Cr(acac)_3}$): δ 259.9 (carbene), 204.0 (trans CO), 199.3 (cis CO's), 152.2 (ipso or para), 146.7 ($\mathit{C}\mathrm{H{=}CH_2}$), 135.8 (ipso or para), 129.4, 119.2 (ortho, meta), 112.6 ($\mathrm{CH{=}}\mathit{C}\mathrm{H_2}$), 75.2 ($\mathrm{N{-}CH_2}$), 42.9 ($\mathrm{NCH_3}$), 38.0 ($\mathit{C}\mathrm{(CH_3)_2}$), 25.1 ($\mathrm{C(}\mathit{C}\mathrm{H_3)_2}$), 20.9 ($\mathrm{Ar}\mathit{C}\mathrm{H_3}$).

For **13**-*E*: ^{1}H NMR (270 MHz, $\mathrm{C_6D_6}$): δ 6.90 (d, J = 8.5 Hz, 2 H), 6.25 (d, J = 8.3 Hz, 2 H), 5.27 (dd, J = 17.5, 11.0 Hz, 1 H, $\mathrm{C}\mathit{H}{=}\mathrm{CH_2}$), 4.75 (d, J = 10.8 Hz, 1 H, $\mathrm{CH{=}C}\mathit{H}\mathrm{H}$), 4.67 (d, J = 17.5 Hz, 1 H, $\mathrm{CH{=}CH}\mathit{H}$), 3.29 (s, 3 H, $\mathrm{NCH_3}$), 2.81 (s, 2 H, $\mathrm{NCH_2}$), 2.01 (s, 3 H, $\mathrm{ArCH_3}$), 0.47 (s, 6 H, $\mathrm{C(CH_3)_2}$). ^{13}C{^{1}H} NMR (50.1 MHz, $\mathrm{C_6D_6}$, 0.09 M $\mathrm{Cr(acac)_3}$): δ 261.5 (carbene), 204.7 (trans CO), 199.2 (cis CO's), 151.0 (ipso or para), 146.1 ($\mathit{C}\mathrm{H{=}CH_2}$), 135.7 (ipso or para), 128.9, 120.7 (ortho, meta), 112.8 ($\mathrm{CH{=}}\mathit{C}\mathrm{H_2}$), 66.3 ($\mathrm{NCH_2}$), 53.9 ($\mathrm{NCH_3}$), 37.5 ($\mathit{C}\mathrm{(CH_3)_2}$), 25.7 ($\mathrm{C(}\mathit{C}\mathrm{H_3)_2}$), 23.2 ($\mathrm{Ar}\mathit{C}\mathrm{H_3}$).

***cis*-Tetracarbonyl[((*Z*)-η^2-*N*-allyl-*N*-methylamino)(*p*-tolyl)carbene]tungsten(0) (14).** A solution of LDA (0.541 mmol) in 3.4 mL of THF was added to a solution of alkene–carbene complex **3** (204 mg, 0.45 mmol) in 40 mL of THF at −72 °C and the solution was allowed to warm to room temperature. The solution was cooled to −72 °C, $\mathrm{CH_3I}$ (40 μL, 0.64 mmol) was added, and the solution warmed to room temperature. Preparative TLC (silica gel, 1:1 $\mathrm{CH_2Cl_2}$–hexane, R_f 0.28) gave **14** (197 mg, 94%) as a yellow crystalline solid, mp 107–108 °C.

---

[35] Burum, D. P.; Ernst, R. R. *J. Magn. Reson.* **1980**, *39*, 163–168. Charles, H. C.; Evans, C. A. "Polarization Transfer Sequences 1. INEPT, Coupled and Decoupled"; Application Note, JEOL Analytical Instruments, Inc., Cranford, NJ 07016 (Jan 1981).

IR (cyclohexane): 2022 (m), 1945 (w), 1937 (s), 1931 (sh), 1910 (s), 1904 (m) $\mathrm{cm^{-1}}$. IR (Nujol): 2021 (m), 1947 (w), 1936 (s), 1928 (sh), 1912 (s), 1904 (m) $\mathrm{cm^{-1}}$. ^{1}H NMR (270 MHz, C_6D_6): δ 6.90 (d, J = 7.7 Hz, 2 H), 6.53 (d, J = 7.7 Hz, 2 H), 3.99 (m, 1 H, $\mathrm{C}\mathit{H}{=}\mathrm{CH_2}$), 3.63 (dd, J = 13.6, 4.8 Hz, 1 H, $\mathrm{NC}\mathit{H}\mathrm{H}$), 3.10 (d, J = 8.6 Hz, 1 H, $\mathrm{CH{=}C}\mathit{H}\mathrm{H}$), 3.00 (d, J = 12.9 Hz, 1 H, $\mathrm{CH{=}CH}\mathit{H}$), 2.92 (dd, J = 13.6, 5.3 Hz, 1 H, $\mathrm{NCH}\mathit{H}$), 2.03 (s, 3 H, $\mathrm{ArC}\mathit{H}_3$), 1.86 (s, 3 H, NCH_3). ^{13}C{^{1}H} NMR (50.1 MHz, CD_2Cl_2, 0.09 M $\mathrm{Cr(acac)_3}$): δ 216.3 (carbene), 211.7, 210.1, 203.4, 203.2 (4 CO's), 146.6, 136.5 (ipso, para), 128.7, 120.6 (ortho, metal), 70.2, 65.1, 59.3 ($\mathrm{CH_2CH{=}CH_2}$), 40.7 (NCH_3), 20.9 ($\mathrm{Ar}\mathit{C}\mathrm{H_3}$).

cis*-Tetracarbonyl[(((*Z*)-η^2-*N*,2,2-trimethyl-3-butenyl)amino)(*p*-tolyl)carbene]tungsten(0) (6) and 1-*p*-Tolyl-2,4,4-trimethyl-2-azabicyclo[3.1.0]hexane (7).** A 2:1 mixture of **13-*Z and **13-*E*** (310 mg, 0.575 mmol) in 15 mL of benzene was sealed in a 45-mL glass tube under vacuum. After 75 h at 99 °C, the tube was opened, benzene was evaporated, and the residue was purified by preparative TLC (silica gel, 1:2 CH_2Cl_2–hexane). Three bands were isolated: R_f 0.50, **13-*Z*** and **13-*E*** (1:3.5; 65 mg, 21%); R_f 0.33, solid **6** (102 mg, 35%, mp 106 °C); R_f 0.12, a pink liquid which after vacuum distillation (45 °C, $\leq 10^{-4}$ mmHg) gave **7** (21.6 mg, 17.5%) as a clear liquid.

For **6**: IR (cyclohexane): 2019 (s), 1932 (s), 1924 (s), 1913 (s), 1898 (sh), 1892 (vs) $\mathrm{cm^{-1}}$. IR (Nujol): 2016 (s), 1927 (s), 1925 (sh), 1915 (s), 1893 (br, vs) $\mathrm{cm^{-1}}$. ^{1}H NMR (270 MHz, C_6D_6): δ 7.00 (m, 2 H), 6.60 (dd, J = 8.2, 2.2 Hz, 1 H), 6.51 (dd, J = 8.2, 2.2 Hz, 1 H), 3.47, 3.42 (AB of ABX, J_{AB} = 9.4 Hz, 2 H, $\mathrm{C}\mathit{H}_{\mathrm{A}}{=}\mathrm{C}\mathit{H}_{\mathrm{B}}\mathrm{H_X}$), 3.15 (X of ABX, J_{AX} = 14.1 Hz, J_{BX} = 0.47 Hz, 1 H), 3.10 (d, J = 13.0 Hz, 1 H, $\mathrm{NC}\mathit{H}\mathrm{H}$), 2.85 (d, J = 13.0 Hz, 1 H, $\mathrm{NCH}\mathit{H}$), 2.23 (s, 3 H, NCH_3, absent in NCD_3), 2.09 (s, 3 H, $\mathrm{ArC}\mathit{H}_3$), 0.83 (s, 3 H, $\mathrm{C(C}\mathit{H}_3\mathrm{)CH_3}$), 0.51 (s, 3 H, $\mathrm{C(CH_3)C}\mathit{H}_3$). Coupling constants and chemical shifts of the ABX pattern of the vinyl protons were obtained by computer simulation of spectra. ^{13}C NMR (50.1 MHz, CD_2Cl_2): δ 263.8 (s, carbene), 209.7 (s, 2 CO's), 202.7 (s, 1 CO), 201.6 (s, 1 CO), 150.1 135.5 (s, s, ipso, para), 128.5, 119.5 (d, d, J = 165, 162 Hz, ortho, meta), 85.5 (d, J = 158 Hz, $\mathit{C}\mathrm{H{=}CH_2}$), 76.7 (t, J = 143 Hz, NCH_2), 56.2 (t, J = 154 Hz, $\mathrm{CH{=}}\mathit{C}\mathrm{H_2}$), 46.2 (q, J = 142 Hz, NCH_3), 37.3 (s, $\mathit{C}\mathrm{(CH_3)_2}$), 29.8, 22.7, 20.4 (q, q, q, J = 127, 130, 125 Hz, $\mathrm{C(}\mathit{C}\mathrm{H_3)_2}$, $\mathrm{Ar}\mathit{C}\mathrm{H_3}$).

Anal. Calcd for $C_{19}H_{21}NO_4W$: C, 44.63; H, 4.11; N, 2.74. Found: 44.73; H, 3.97; N, 2.76.

For **7**: IR (neat): 1520 (s), 1488 (w), 1365 (m), 1205 (m), 1090 (m), 811 (s) $\mathrm{cm^{-1}}$. ^{1}H NMR (270 MHz, C_6D_6): δ 7.44 (d, J = 8.1 Hz, 2 H), 7.05 (d, J = 7.7 Hz, 2 H), 2.61 (d, J = 9.6 Hz, 1 H, $\mathrm{NC}\mathit{H}\mathrm{H}$), 2.15 (s, 3 H, $\mathrm{ArC}\mathit{H}_3$), 2.13 (s, 3 H, NCH_3 absent in NCD_3), 1.67 (d, J = 9.6 Hz, $\mathrm{NCH}\mathit{H}$), 1.22 (s, 3 H, $\mathrm{C(C}\mathit{H}_3\mathrm{)CH_3}$), 1.00 (dd, J = 8.3, 4.6 Hz, 1 H, cyclopropyl CH), 0.93 (s, 3 H, $\mathrm{C(CH_3)C}\mathit{H}_3$), 0.89 (dd, J = 5.9, 4.6 Hz, 1 H, cyclopropyl $\mathrm{C}\mathit{H}\mathrm{H}$, endo), 0.79 (dd, J = 8.5, 5.9 Hz, 1 H, cyclopropyl $\mathrm{CH}\mathit{H}$ exo). ^{13}C NMR (50.1 MHz, acetone-d_6): δ 139.8, 136.1 (s, ipso, para), 129.5, 127.9 (d, d, J = 161, 160 Hz, ortho, meta), 65.6 (t, J = 138 Hz, NCH_2), 54.8 (s, cyclopropyl N–C), 39.3 (s, $\mathit{C}\mathrm{(CH_3)_2}$), 38.1, 37.9 (q, q, J = 133, 133 Hz, NCH_3, $\mathrm{C(}\mathit{C}\mathrm{H_3)(CH_3)}$), 28.5 (d, J = 136 Hz, cyclopropyl C–H) 24.1, 21.1 (q, q, J = 128, 128 Hz, $\mathrm{C(CH_3)}\mathit{C}\mathrm{H_3}$, $\mathrm{Ar}\mathit{C}\mathrm{H_3}$), 5.3 (t, J = 137 Hz, cyclopropyl CH_2).

Anal. Calcd for $C_{15}H_{21}N$: C, 83.73; H, 9.76; N, 6.51. Found: C, 83.42; H, 10.03; N, 6.31.

X-ray Structural Determination. A single crystal of **6** obtained by slow cooling of a saturated xylene–pentane (1:3) solution was mounted on a glass fiber and coated with epoxy cement to prevent contact with the atmosphere. Preliminary examination and collection of the diffraction data were carried out on a Syntex-Nicolet $\mathrm{P\bar{1}}$ diffractometer equipped with a graphite monochromated Mo Kα radiation source and a modified LT-1 low-temperature device. Structure amplitudes and their standard deviations were calculated from the intensity data by procedures similar to those described previously.[36] Crystal data and details of the intensity data collection are given in Table III.

The structure was solved from the Patterson map which revealed the positions of both independent tungsten atoms (the Patterson map was inconsistent with the alternate space group choice of $P2_1/m$, thus confining the space group to be $P2_1$). A series of difference electron density maps revealed the other non-hydrogen atoms. After several cycles of least-squares refinement[37] a number of distances and angles, particularly in the region of the alkene in molecule 2, were unrealistic. Examination of difference electron density maps suggested that the structure was disordered due to transposition of the conformations of the chelate rings of the two independent molecules (see Results). The transpositions occur in such a way that most of the atoms of the minor component nearly overlap the atoms of the major component. The tolyl methyl carbon atoms and the atoms in the alkene region were sufficiently separated to be refined. The initial positions for these atoms of the minor component were obtained by matching the geometry of the corresponding atoms of the major component to the difference map. The occupancies of the major and minor components were set at 0.7 and 0.3 on the basis of relative peak heights in the Fourier maps. The model was refined by using constrained least-squares refinement.[38,39] Slack constraints were placed on the corresponding distances in the alkene regions; no constraints were placed on angles. The atoms of the major component were refined anisotropically and the atoms of the minor components were refined isotropically. In the final cycles of refinements the constraints were relaxed. The final discrepancy indices were $R_1 = \sum||F_o| - |F_c||/\sum|F_o| = 0.038$ and $R_2 = [\sum w(F_o - F_c)^2/\sum w(F_o)^2]^{1/2} = 0.074$. The estimated standard deviation of an observation of unit weight was 2.04 and the final data/variable ratio was 8.62. The only significant peaks on the final electron density difference map are near the tungsten atoms. Selected interatomic distances and angles are given in Tables I and II. Atomic coordinates, thermal parameters, and a listing of $10|F_o|^2$ and $10|F_c|^2$ are given as supplementary material.

Table III. Summary of Crystal Data and Intensity Collection

empirical formula	$C_{19}H_{21}NO_4W$
crystal dimensions, mm	0.4 × 0.5 × 0.7
temp, K	183 ± 5
cell parameters	
a, Å	10.287 (3)
b, Å	11.651 (3)
c, Å	16.319 (5)
β, deg	98.83 (2)
space group	$P2_1$
Z	4
density	
calcd, g/cm^3	1.76
obsd, g/cm^3	1.70
absorption correction	ψ curve
coeff, μ, cm^{-1}	57.3
scan range	
deg below $2\theta_{\mathrm{K}\alpha_1}$	0.9
deg below $2\theta_{\mathrm{K}\alpha_2}$	0.9
scan speed, deg/min	2.0–24.0
scan type	θ–2θ
2θ limits, deg	3.5–54.9
unique data $F_o > 3\sigma(F_o)$	4295

Tetracarbonyl(trimethylphosphine)[(((*Z*)-*N*,2,2-trimethyl-3-butenyl)amino)(*p*-tolyl)carbene]tungsten(0) (15-*Z* and 15-*E*). PMe_3 (268 mL, 9.17 mmHg, 0.132 mmol) was vacuum transferred into a solution of **5** (33.6 mg, 0.065 mmol) in 15 mL of xylene. After the reaction was stirred for 1 h at room temperature, xylene and excess PMe_3 were evaporated. Preparative TLC gave **15-*Z*** (30 mg, 78%). IR (cyclohexane): 2008 (m), 1919 (s), 1889 (vs), 1860 (s) $\mathrm{cm^{-1}}$. ^{1}H NMR (270 MHz, C_6D_6): δ 6.97 (d, J = 8.3 Hz, 2 H), 6.58 (d, J = 8.1 Hz, 2 H), 5.77 (dd, J = 17.3, 10.8 Hz, 1 H $\mathrm{C}\mathit{H}{=}\mathrm{CH_2}$), 4.85 (dd, J = 10.7, 1.1 Hz, 1 H, $\mathrm{CH{=}CH}\mathit{H}$), 4.82 (dd, J = 17.4, 1.2 Hz, 1 H, $\mathrm{CH{=}C}\mathit{H}\mathrm{H}$), 4.03 (s, 2 H, NCH_2), 2.36 (br s, 3 H, NCH_3), 2.10 (s, 3 H, $\mathrm{ArC}\mathit{H}_3$), 1.16 (s, 6 H, $\mathrm{C(C}\mathit{H}_3\mathrm{)_2}$), 1.14 (d, J_{PH} = 7.3 Hz, 9 H, $\mathrm{P(CH_3)_3}$). ^{13}C NMR (50.1 MHz, CD_2Cl_2): δ 266.6 (s, carbene), 211.3 (s, CO), 209.2 (d, J_{PC} = 25.7 Hz, CO trans to PMe_3), 204.2 (s, 2 CO's), 152.9 (s, ipso or para), 147.4 (d, J = 151 Hz, $\mathit{C}\mathrm{H{=}CH_2}$), 134.9 (s, ipso or para), 128.5 and 119.2 (d, d, J = 161, 158 Hz, ortho and meta) 112.0 (t, J = 156 Hz, $\mathrm{CH{=}}\mathit{C}\mathrm{H_2}$), 74.5 (t, J = 138 Hz, NCH_2), 42.9 (q, J = 123 Hz, NCH_3), 38.2 (s, $\mathit{C}\mathrm{(CH_3)_2}$), 23.6 (q, J = 135 Hz, $\mathrm{C(}\mathit{C}\mathrm{H_3)_2}$), 20.5 (q, J = 125 Hz, $\mathrm{Ar}\mathit{C}\mathrm{H_3}$), 20.1 (qd, J_{CH} = 132 Hz, J_{PC} = 26.0 Hz, $\mathrm{P(}\mathit{C}\mathrm{H_3)_3}$).

Heating solutions of **15-*Z*** results in isomerization about the carbene carbon–nitrogen partial double bond giving mixtures of **15-*Z*** and **15-*E***. For **15-*E***, ^{1}H NMR (270 MHz, C_6D_6), δ 6.94 (d, J = 8.0 Hz, 2 H), 6.71 (d, J = 7.9 Hz, 2 H), 5.42 (dd, J = 17.5, 10.7 Hz, 1 H, $\mathrm{C}\mathit{H}{=}\mathrm{CH_2}$), 4.82 (dd, J = 10.7 0.8 Hz, 1 H, $\mathrm{CH{=}CH}\mathit{H}$), 4.76 (dd, J = 17.5, 0.9 Hz, 1 H, $\mathrm{CH{=}C}\mathit{H}\mathrm{H}$), 3.44 (s, 3 H, NCH_3), 2.96 (s, 2 H, NCH_2), 2.07 (s, 3

---

(36) Haller, K. J.; Enemark, J. H. *Inorg. Chem.* **1978**, *17*, 3552–8.

(37) Atomic form factor were from Cromer, D. T.; Mann, J. B. "International Tables for X-Ray Crystallography"; Kynoch Press: Birmingham, England, 1974; Vol. 4, pp 99–101, Table 2.2B. Real and imaginary corrections for anomalous dispersion in the scattering factor of the tungsten atoms were from: Cromer, D. T.; Liberman, D. J. *J. Chem. Phys.* **1970**, *53*, 1891–98.

(38) Rae, A. D. "RAELS, A Comprehensive Least-Square Program"; University of New South Wales, Kensington, 1976. Adapted for a Harris/7 computer by A. D. Rae, University of Wisconsin—Madison, 1980.

(39) Maj, J. J.; Rae, A. D.; Dahl, L. F. *J. Am. Chem. Soc.* **1982**, *104*, 3054–3063.

3764 J. Am. Chem. Soc. 1984, 106, 3764-3767

H, ArCH_3), 1.15 (d, $J = 7.2$ Hz, 9 H, $P(CH_3)_3$), 0.61 (s, 6 H, $C(CH_3)_2$).

Acknowledgment. Support from the National Science Foundation is gratefully acknowledged.

Registry No. 3, 77310-69-1; **5**, 80975-94-6; **6**, 90245-82-2; **7**, 90245-88-8; **8**, 90245-89-9; **9**, 41405-16-7; **10**-*Z*, 90245-83-3; **10**-*E*, 90319-42-9; **11**, 90245-90-2; **13**-*Z*, 90245-84-4; **13**-*E*, 90319-43-0; **14**, 90245-85-5; **15**-*Z*, 90245-86-6; **15**-*E*, 90319-44-1; **18**-*Z*, 90245-87-7; **18**-*E*, 90319-45-2; **19**, 90245-81-1; *trans*-$W(CO)_4(PPh_3)_2$, 16743-03-6; $(CO)_5W(OCH_3)C_6H_4$-*p*-CH_3, 38669-72-6; 3-butenenitrile, 109-75-1.

Supplementary Material Available: Atomic coordinates (Table IV), thermal parameters (Table V), and a listing of structure factor amplitudes (Table VI) for **6** (21 pages). Ordering information is given on any current masthead page.

Photochemistry of Hexacyanocobaltate(III) in Haloalkanes

Steven J. Milder, Harry B. Gray,* and Vincent M. Miskowski*

Contribution No. 6911 from the Arthur Amos Noyes Laboratory, California Institute of Technology, Pasadena, California 91125, and the Jet Propulsion Laboratory, Pasadena, California 91109. *Received September 19, 1983*

Abstract: Haloalkane complexes of pentacyanocobaltate(III) are produced in high quantum yield (~0.3) by irradiating $(TBA)_3[Co(CN)_6]$ in neat haloalkane solvents. The CH_2Cl_2 and 1,3-dibromopropane complexes have their $^1A_1 \rightarrow {}^1E^a$ ligand field transitions at 405 and 415 nm, respectively. These complexes have a rise time of ≤ 10 ns and decay by second-order kinetics with a rate constant of 1.5×10^3 M^{-1} s^{-1} in CH_2Cl_2; the reaction was confirmed as recombination with photolytically released CN^- by observation of pseudo-first-order kinetics in the presence of added CN^-. Scavenging studies with CH_3CN demonstrated rate saturation for formation of $Co(CN)_5(NCCH_3)^{2-}$ at high [CH_3CN], which is interpreted in terms of a limiting dissociative mechanism for reaction of the CH_2Cl_2 complex. The dissociation rate was found to be 1.6 (4) $\times$ 10^3 s^{-1} and competition ratios for reaction with ligand L vs. CH_2Cl_2 were evaluated to be 135 (25) and 15 (3) for L = CH_3CN and CN^-, respectively. High CH_3CN concentrations also resulted in decrease of the prompt absorbance of the CH_2Cl_2 complex, and a theoretical fit of the [CH_3CN] dependence indicated a competition ratio (CH_3CN vs. CH_2Cl_2) consistent with a photochemical precursor identical with the thermal substitution intermediate, which is assumed to be singlet square-pyramidal $Co(CN)_5^{2-}$. Detailed comparisons are made to thermal and photochemical substitutions in other solvents.

The lowest excited state ($^3T_{1g}$) of $Co(CN)_6^{3-}$ in its crystalline potassium salt exhibits lifetimes of 8 and 680 μs at room temperature and 77 K, respectively.[1] In aqueous solution, in contrast, the triplet lifetime is only 2.6 ns at room temperature,[2] and the photoaquation yield is 0.31,[3,4] indicating that photosubstitution processes dominate excited-state decay.

Because there is a great interest in photochemically induced transient species as sources of catalytic reactivity, we were curious as to what the photophysical behavior of $Co(CN)_6^{3-}$ would be in a very poorly ligating solvent such as a haloalkane. As the photosubstitution had been suggested[5] to have interchange character[6] in aqueous solution, it seemed possible that the excited-state lifetime might be greatly increased. The triplet yield upon singlet excitation has recently been established[7] as unity.

If photosubstitution nonetheless dominated, it seemed clear that weak solvent complexes would be formed, as solvents as weakly ligating as alkanes form well-defined complexes upon photolysis of isoelectronic $M(CO)_6$ complexes.[8,9] Such weak complexes also present the possibility of useful reactivity.

The tetrabutylammonium (TBA) salt of $Co(CN)_6^{3-}$ was first reported many years ago;[10] it has significant solubility in polar organic solvents. We have performed detailed studies of its photophysical behavior in halocarbon solvents, concentrating upon the solvent CH_2Cl_2, and report our results herein.

Experimental Section

Static photolyses were performed with a 1000-W Hg lamp filtered to isolate the 313-nm line. The photoaquation of $Co(CN)_6^{3-}$ ($\phi = 0.31$)[3,4] was used as the actinometer.

Conventional flash photolysis was performed with an apparatus described elsewhere.[11] The xenon flash lamp was typically fired with 240-J energy (pulse width ~20 μs) and was Pyrex filtered. In most experiments, the analyzing light beam was filtered so as to minimize light absorption by starting material.

Laser (nanosecond) flash photolysis experiments employed the third harmonic (353 nm) of a Nd/glass laser[12] in the laboratory of Professor Arthur Adamson at the University of Southern California.

The salt $(TBA)_3[Co(CN)_6]$ was prepared either by the method of ref 10 or by mixing saturated solutions of $(TBA)ClO_4$ in methanol and $K_3[Co(CN)_6]$ in H_2O, with the latter in stoichiometric excess, filtering off precipitated $KClO_4$, and, after evaporation of the filtrate, recrystallizing from CH_2Cl_2.

(TBA)CN was obtained from Fluka and used as received. This exceedingly hygroscopic material was handled under a N_2 atmosphere in a glovebag. 1,3-Dibromopropane (DBP) from Aldrich was dried over P_2O_5, distilled, and degassed by five freeze-pump-thaw (FPT) cycles.

---

(1) Wolpl, A.; Oelkrug, D. *Ber. Bunsenges, Phys. Chem.* **1975**, *79*, 394.

(2) Conti, C.; Castelli, F.; Forster, L. S. *J. Phys. Chem.* **1979**, *83*, 2371.

(3) Balzani, V.; Carasitti, V. "Photochemistry of Coordination Compounds"; Academic Press: New York, 1970; p 219.

(4) Nakamaru, K.; Jin, K.; Tazawa, A.; Kanno, M. *Bull. Chem. Soc. Jpn.* **1975**, *48*, 3486.

(5) Wrighton, M.; Hammond, G. S.; Gray, H. B. *J. Am. Chem. Soc.* **1971**, *93*, 5254.

(6) Langford, C. H.; Gray, H. B. "Ligand Substitution Processes"; W. A. Benjamin: Reading, MA, 1974.

(7) Nishazawa, M.; Ford, P, P. C. *Inorg. Chem.* **1981**, *20*, 294.

(8) (a) Bonneau, R.; Kelly, J. M. *J. Am. Chem. Soc.* **1980**, *102*, 1220. (b) Perutz, R. N.; Turner, J. J. *Ibid.* **1975**, *97*, 4791.

(9) Lees, A. J.; Adamson, A. W. *Inorg. Chem.* **1981**, *20*, 4381.

(10) Alexander, J. J.; Gray, H. B. *J. Am. Chem. Soc.* **1968**, *90*, 4260.

(11) Milder, S. J.; Goldbeck, R. A.; Kliger, D. S.; Gray, H. B. *J. Am. Chem. Soc.* **1980**, *102*, 6761.

(12) Fukuda, R.; Waters, R. T.; Mäcke, H.; Adamson, A. W. *J. Phys. Chem.* **1979**, *83*, 2097.